

## Frustrated Lewis Pairs

# The Chemistry of a Non-Interacting Vicinal Frustrated Phosphane/Borane Lewis Pair

Lisa-Maria Elmer,<sup>[a]</sup> Gerald Kehr,<sup>[a]</sup> Constantin G. Daniliuc,<sup>[a]</sup> Melanie Siedow,<sup>[b]</sup> Hellmut Eckert,<sup>[b, d]</sup> Matthias Tesch,<sup>[a]</sup> Armido Studer,<sup>[a]</sup> Kamille Williams,<sup>[c]</sup> Timothy H. Warren,<sup>[c]</sup> and Gerhard Erker<sup>\*[a]</sup>

Dedicated to Professor Rolf Gleiter on the occasion of his 80th birthday

**Abstract:** The dimesitylphosphinocyclopentene/HB(C<sub>6</sub>F<sub>5</sub>)<sub>2</sub>-derived vicinal *trans*-1,2-P/B frustrated Lewis pair (FLP) **4** shows no direct phosphane–borane interaction. Toward some reagents it behaves similar to an intermolecular FLP; it cleaves dihydrogen, deprotonates terminal alkynes, and adds to organic carbonyl compounds including CO<sub>2</sub>. It shows typical intramolecular FLP reaction modes (cooperative 1,1-additions) to mesityl azide, to carbon monoxide, and to NO. The latter reaction yields a persistent P/B FLPNO ni-

troxide radical, which undergoes H-atom abstraction reactions. The FLP **4** serves as a template for the CO reduction by [HB(C<sub>6</sub>F<sub>5</sub>)<sub>2</sub>] to generate a FLP- $\eta^2$ -formylborane. The formylborane moiety is removed from the FLP template by reaction with pyridine to yield a genuine pyridine stabilized formylborane that undergoes characteristic borane carbaldehyde reactions (Wittig olefination, imine formation). Most new products were characterized by X-ray diffraction.

## Introduction

Frustrated Lewis pair (FLP) chemistry has seen some remarkable development in recent years. An increasing number of FLP types has led to many new examples of small molecule binding and/or activation, and sometimes to new reactions.<sup>[1,2]</sup> Usually the Lewis acids and bases in FLPs are effectively hindered from the usual neutralizing adduct formation by attaching very bulky substituents at their core atoms. This can lead to active intermolecular frustrated Lewis pairs.<sup>[3]</sup> Their reaction with added reagents in solution is thought to initially involve the formation of encounter complexes between the FLP components<sup>[4]</sup> from which the actual FLP reaction then can take place. Various types of intermolecular FLPs have successfully

been employed in such reactions, for example, in dihydrogen splitting and/or hydrogenation catalysis.<sup>[5–7]</sup>

In principle the reaction of intramolecular FLPs is less complex since here the Lewis acid and Lewis base components are connected by a linker in a single molecule and, therefore, a bimolecular reaction can just take place with an added substrate.<sup>[8–10]</sup> Various types of bridging frameworks have successfully been used for generating active intramolecular frustrated Lewis pairs, among them many vicinal P/B or N/B FLPs.<sup>[11]</sup>

However, here internal interaction between the FLP Lewis acid and base components of various strengths may (and often does) provide a serious complication. In such cases one assumes efficient opening and closing of the LA/LB contact in a rapid pre-equilibrium before the actual FLP reaction can occur from the active open isomer.<sup>[12]</sup>

There are actually some intramolecular vicinal FLPs that do not show a direct internal Lewis acid–base interaction. This can be due to extreme steric hindrance as it is demonstrated by Repo's N/B FLP pair **1** (interacting, closed structure) and **2** (non-interacting, open)<sup>[10b]</sup> or it can be caused by a special geometric orientation of the respective groups at a suitable framework (Scheme 1). The norbornane-derived *exo*-B(C<sub>6</sub>F<sub>5</sub>)<sub>2</sub>/*endo*-PMes<sub>2</sub> FLP **3** is an example (P···B separation: 3.878(1) Å).<sup>[13]</sup> However, the very reactive P/B FLP **3** is not too convenient to make; therefore, we had looked for alternatives and found that the simple *trans*-1,2-B(C<sub>6</sub>F<sub>5</sub>)<sub>2</sub>/PMes<sub>2</sub> arrangement at the cyclopentane ring in **4** provided a solution. It is an open system and as such might show structural, spectroscopic, and chemical features that can either be reminiscent of those of the many intermolecular FLP examples or be specific to vicinal in-

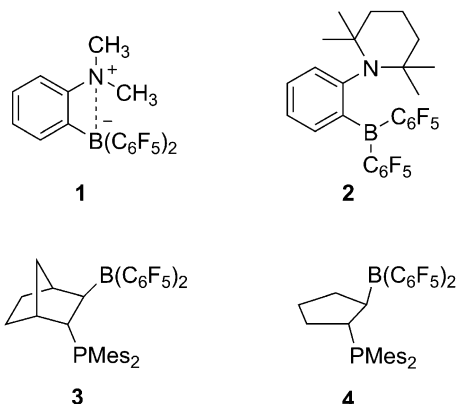
[a] Dr. L.-M. Elmer, Dr. G. Kehr, Dr. C. G. Daniliuc, M. Tesch, Prof. Dr. A. Studer, Prof. Dr. G. Erker  
Organisch-Chemisches Institut, Universität Münster  
Corrensstraße 40, 48149 Münster (Germany)  
E-mail: erker@uni-muenster.de

[b] M. Siedow, Prof. Dr. H. Eckert  
Institut für Physikalische Chemie, Universität Münster  
Corrensstraße 28/30, 48149 Münster (Germany)

[c] K. Williams, Prof. Dr. T. H. Warren  
Georgetown University, Department of Chemistry  
Box 571227, Washington DC 20057-1227 (USA)

[d] Prof. Dr. H. Eckert  
Instituto de Física São Carlos, Universidade de São Paulo, CP 369  
São Carlos, SP, 13560-970 (Brasil)

Supporting information for this article can be found under  
<http://dx.doi.org/10.1002/chem.201603954>.



**Scheme 1.** Open and closed vicinal N/B and P/B frustrated Lewis pairs.

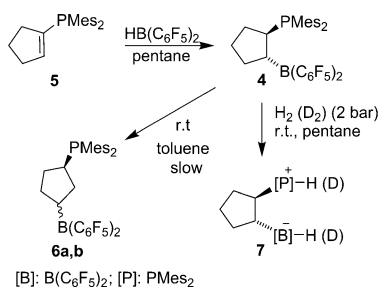
tramolecular systems. Our results on the FLP chemistry of the open, non-internally stabilized FLP system **4** will be described and discussed in this account.

## Results and Discussion

## Synthesis and characterization of the vicinal P/B FLP 4

We prepared the cyclopentane-derived P/B frustrated Lewis pair **4** starting from dimesitylphosphinocyclopentene (**5**). This in turn was conveniently prepared by treatment of cyclopentanone with  $\text{PCl}_5$  followed by lithiation of the resulting chlorocyclopentene and reaction with  $\text{Mes}_2\text{PCl}$ .<sup>[14]</sup> The cyclopentenylphosphane **5** was characterized by X-ray diffraction (for details see the Supporting Information).

Hydroboration of compound **5** with Piers' borane [ $\text{HB}(\text{C}_6\text{F}_5)_2$ ] is fast.<sup>[15]</sup> In solvents such as toluene, dichloromethane, or pentane, the reaction is practically complete within a few minutes, giving a yellow solution of the P/B FLP **4**. We prepared **4** on a preparative scale by reacting **5** with  $\text{HB}(\text{C}_6\text{F}_5)_2$  in pentane at room temperature and then crystallized the product at  $-40^\circ\text{C}$  to give **4** in 69% yield (Scheme 2).



**Scheme 2.** Formation of the P/B FLP 4 and its reaction with dihydrogen.

The X-ray crystal structure analysis (Figure 1) showed the presence of the bulky  $B(C_6F_5)_2$  and  $PMes_2$  functionalities in a *trans*-1,2-arrangement at the cyclopentane derived framework. The B/P separation is large ( $3.84 \text{ \AA}$ ,  $\theta$  P1-C1-C2-B1 =

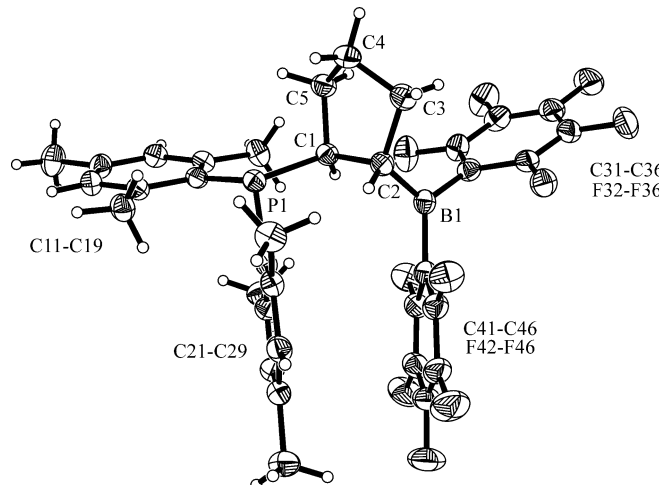


**Figure 1.** Molecular structure of the P/B FLP 4 (ellipsoids are set at 30% probability). Selected bond lengths [Å] and angles [°]: P1–C1: 1.862(2), C1–C2: 1.588(2), C2–B1: 1.541(3), C2–C3: 1.547(3), C3–C4: 1.516(3), C4–C5: 1.519(3), C5–C1: 1.546(3), C11–P1–C1: 110.0(1), C2–B1–C31: 120.3(2), P1–C1–C2–B1: 125.0(1),  $\Sigma B_{ccc}$ : 360.0,  $\Sigma P_{ccc}$ : 321.2, P1···B1: 3.84.

$125.0(1)^\circ$ ), so that we assume that there is no direct P–B interaction in this frustrated Lewis pair. Consequently, the boron atom is planar-tricoordinate ( $\Sigma B1^{CCC} = 360.0^\circ$ ); the phosphorus atom features the typical trigonal pyramidal coordination geometry ( $\Sigma P1^{CCC} = 321.2^\circ$ ). We note that the C41–C46 and the C21–C29  $C_6F_5$ /mesityl arene pair at B1 and P1 are oriented close to parallel (angle between the planes:  $4.4^\circ$ ) with a distance between the centroids of the planes of ca.  $3.6\text{ \AA}$ . The cyclopentane framework in **4** shows a distorted envelope conformation.

In solution, compound **4** shows a  $^{11}\text{B}$  NMR signal at  $\delta = 76.9$  ppm, which is typical for a strongly Lewis acidic planar-tricoordinate  $\text{RB}(\text{C}_6\text{F}_5)_2$  borane. It shows three  $^{19}\text{F}$  NMR resonances with  $\Delta\delta^{19}\text{F}_{p,m} = 11.5$  ppm. The  $^{31}\text{P}$  NMR resonance of compound **4** is at  $\delta = -12.5$  ppm.

Compound **4** is thermally sensitive, which is probably due to a subsequent isomerization by means of retro-hydroboration/hydroboration sequences. Within several hours at room temperature this results in the formation of a mixture of **4** and two isomers **6a,b**; these were not positively identified, but we assume that they are to be regarded as the respective *cis*- and *trans*-1,3-disubstituted isomers. After heating for 5 h at 70 °C in [D<sub>8</sub>]toluene a mixture of **4:6a:6b** in a ratio of ca. 1:1.6:2.5 was formed. To avoid complication due to the subsequent isomerization reaction we always generated the P/B FLP **4** by reacting **5** with HB(C<sub>6</sub>F<sub>5</sub>)<sub>2</sub> for a few minutes in the respective solvent and used these freshly prepared samples of **4** (after NMR control) for the subsequent FLP reactions described below.

Compound **4** is a reactive FLP. It reacted with dihydrogen under mild conditions (2 bar, room temperature) to give the product of heterolytic H<sub>2</sub>-splitting.<sup>[1,2]</sup> From the respective pentane solution we isolated the [P]H<sup>+</sup>/[B]H<sup>-</sup> product **7** as a white solid in 68% yield. Single crystals for the X-ray crystal structure analysis were obtained from dichloromethane/pentane by the diffusion method. It shows a *trans*-1,2-arrangement of the

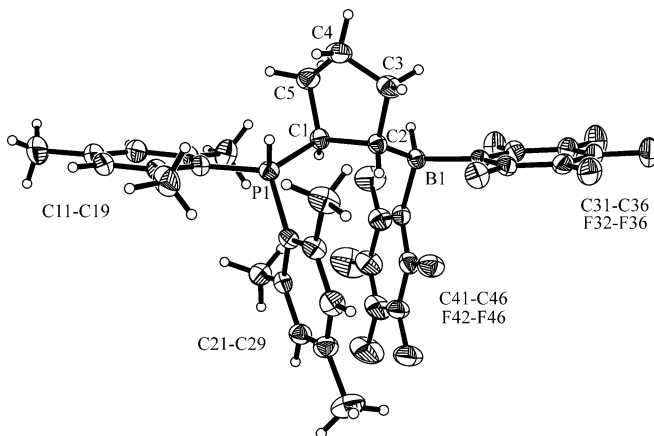


**Figure 2.** A view of the molecular structure of the  $\text{PH}^+/\text{BH}^-$  zwitterion **7** (ellipsoids are set at 30% probability). Selected bond lengths [ $\text{\AA}$ ] and angles [ $^\circ$ ]: P1–C1: 1.813(3), C1–C2: 1.564(4), C2–B1: 1.635(4), C11–P1–C1: 116.8(2), C2–B1–C31: 114.5(2), P1–C1–C2–B1: 137.8,  $\Sigma\text{B}^{\text{CCC}}$ : 334.2,  $\Sigma\text{P}^{\text{CCC}}$ : 344.4, P1–B1: 4.08.

$\text{P(H)Mes}_2^+$  and  $\text{BH}(\text{C}_6\text{F}_5)_2^-$  substituents at the five-membered carbocyclic framework (see Figure 2). The P/B separation in compound **7** is large at 4.08  $\text{\AA}$ . Both the phosphorus and the boron atom now have a hydrogen atom attached, which are also oriented away from each other (P–H/H–B separation: 5.06  $\text{\AA}$ ). The boron coordination geometry in the zwitterionic product **7** is pseudo-tetrahedral ( $\Sigma\text{B}^{\text{CCC}}=334.2^\circ$ ).

The  $^{11}\text{B}$  NMR signal of compound **7** is at  $\delta=-19.2$  ppm. It shows coupling to the attached hydrogen ( $^1J_{\text{BH}} \approx 90$  Hz). The  $^{31}\text{P}$  NMR resonance is at  $\delta=-3.2$  ppm. It shows the typical large  $^1J_{\text{PH}}=463$  Hz coupling constant (corresponding  $^1\text{H}$  NMR [P]–H signal at  $\delta=7.14$  ppm). Owing to the molecular chirality, both the pairs of mesityl substituents at phosphorus and the  $\text{C}_6\text{F}_5$  substituents at the tetracoordinated boron atom are diastereotopic. The  $\Delta\delta^{19}\text{F}_{p,m}$  separation of each  $\text{C}_6\text{F}_5$  substituent is small (2.0 and 2.8).

Reaction of the P/B FLP **4** with  $\text{D}_2$  (1.7 bar) under similar conditions gave the zwitterionic  $[\text{P}]^{\text{D}}^+/\text{[B]}^{\text{D}}^-$  product **7-D<sub>2</sub>**. It showed a  $[\text{P}]^{\text{D}}^+$  doublet in the  $^2\text{H}$  NMR spectrum ( $\delta=7.15$  ppm,  $^1J_{\text{PD}}=71.2$  Hz) and a broad  $[\text{B}]^{\text{D}}^-$  signal at  $\delta=2.67$  ppm. The  $^{11}\text{B}$  NMR resonance of **7-D<sub>2</sub>** was located at  $\delta=-19.3$  ppm. The  $^{31}\text{P}$  NMR resonance is broadened, but features a 1:1:1 equal intensity triplet upon proton decoupling ( $\delta=-3.7$  ppm,  $^1J_{\text{PD}} \approx 71$  Hz in dichloromethane).

Both the P/B FLP **4** and the  $[\text{P}]^{\text{H}}^+/\text{[B]}^{\text{H}}^-$  hydrogen activation product **7** have been used as metal-free hydrogenation catalysts for typical organic substrates.<sup>[16]</sup> However, their performance was not optimal as compared to other P/B FLPs, probably because of complications due to the above mentioned isomerization processes that may take place under the applied hydrogenation conditions (for details see the Supporting Information).

### Addition reactions at the boron Lewis acid

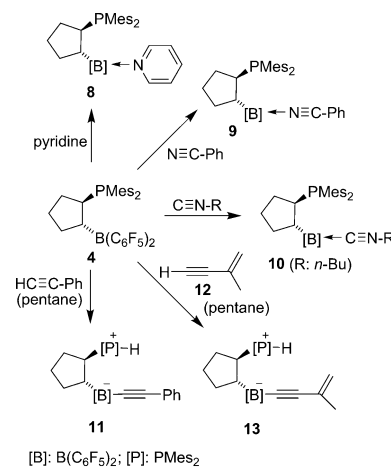
The reactions of **4** with a few donor reagents and with terminal alkynes proceeded similarly as they have often been ob-

served with both intra- and intermolecular FLPs. Treatment of **4** with pyridine<sup>[17]</sup> ( $\text{CH}_2\text{Cl}_2/\text{pentane}$ ) gave the crystalline adduct **8** in 75% yield (Scheme 3). The X-ray crystal structure analysis showed that the pyridine donor had just added to the  $\text{B}(\text{C}_6\text{F}_5)_2$  group ( $\text{B1–N1}$  1.631(8)  $\text{\AA}$ ,  $\Sigma\text{B1}^{\text{CCC}}=336.7^\circ$ ,  $\theta$  P1–C1–C2–B1 153.3(4)° (for details see the Supporting Information).

Compound **4** also cleanly formed a borane adduct **9** with benzonitrile. It shows a  $^{11}\text{B}$  NMR resonance at  $\delta=-4.7$  ppm ( $^{31}\text{P}$ :  $\delta=-16.2$  ppm). The X-ray crystal structure analysis of **9** features a  $-\text{C}\equiv\text{N}$  bond length ( $\text{C6–N1}$  1.141(3)  $\text{\AA}$ ) that is slightly longer than the one observed in free benzonitrile (1.138  $\text{\AA}$ ). This typical feature of a Lewis acid adduct of a  $\text{RC}\equiv\text{N}$  donor is complemented by the observed shifting of the IR  $\tilde{\nu}$ ( $\text{C}\equiv\text{N}$ ) stretching band in **9** to larger wavenumbers ( $\tilde{\nu}=2308$   $\text{cm}^{-1}$ ) relative to the free benzonitrile ( $\tilde{\nu}=2230$   $\text{cm}^{-1}$ ).<sup>[18]</sup> For further details about the characterization of the adduct **9** see the Supporting Information.

The FLP **4** also forms the respective borane Lewis acid adduct with *n*-butyl isocyanide. The adduct **10** was isolated in 88% yield and characterized by X-ray diffraction (for details see the Supporting Information). It also shows a carbon-nitrogen triple-bond length of the isonitrile end-on bonded to the strong boron Lewis acid of 1.146(7)  $\text{\AA}$  ( $\text{N1–C6}$ ) and an IR  $\tilde{\nu}$ ( $\text{C}\equiv\text{N}$ ) stretch of  $\tilde{\nu}=2297$   $\text{cm}^{-1}$ .

We reacted the FLP **4** with phenylacetylene (Scheme 3) in *n*-pentane solution and isolated the product **11** as a colorless solid in 88% yield. Compound **11** was characterized by X-ray diffraction. It shows that the terminal alkyne was deprotonated by the phosphane base of the FLP **4** and the remaining acetylide moiety bonded to the borane Lewis acid (Figure 3).<sup>[18, 19]</sup> Consequently, compound **11** features a *trans*-1,2-arrangement of the  $\text{P(H)Mes}_2^+$  and  $\text{B}(\text{C}_6\text{F}_5)_2\text{—C}\equiv\text{C–Ph}^-$  substituents at its five-membered carbocyclic core.



**Scheme 3.** Reactions of the P/B FLP **4** with donor molecules and with terminal alkynes.

In solution, compound **11** shows a  $^{11}\text{B}$  NMR signal at  $\delta=-16.5$  ppm and a  $^{31}\text{P}$  NMR resonance at  $\delta=0.0$  ppm with the typical large  $^1J_{\text{PH}}$  coupling constant of ca. 470 Hz. The alkynyl unit at boron shows  $^{13}\text{C}$  NMR signals at  $\delta=109.7$  ppm ([B]–C≡)

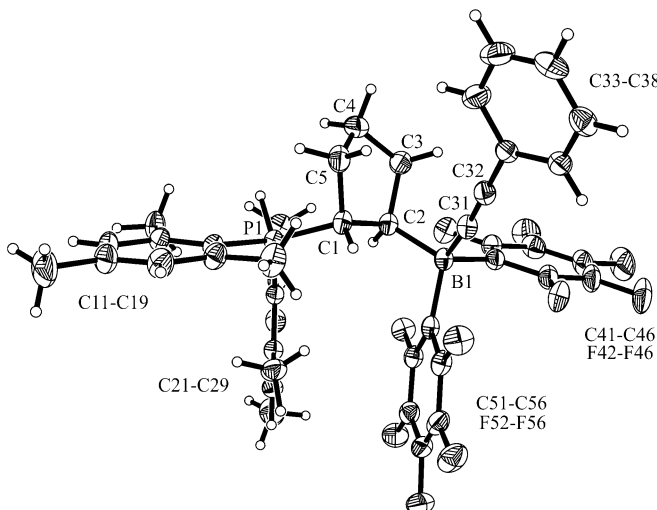


**Figure 3.** Molecular structure of compound 11 (ellipsoids are set at 30% probability). Selected bond lengths [ $\text{\AA}$ ] and angles [ $^\circ$ ]: P1–C1: 1.820(3), C1–C2: 1.564(4), C2–B1: 1.652(4), B1–C31: 1.596(4), C31–C32: 1.209(4), C32–C33: 1.442(4), C32–C31–B1: 169.5(3), C31–C32–C33: 178.9(3), C31–B1–C2: 105.4(2), C11–P1–C1: 117.6(1), C2–B1–C41: 115.1(2), P1–C1–C2–B1: -132.9(2),  $\Sigma B^{C_2C_41C_51}$ : 330.0,  $\Sigma P^{CCC}$ : 344.5.

and  $\delta = 95.3 \text{ ppm} (\equiv \text{C}-\text{Ph})$ , respectively. Both the pairs of mesityl groups at phosphorus and the  $\text{C}_6\text{F}_5$  groups at boron in compound 11 are diastereotopic and thus show 1:1 intensity pairs of the respective NMR resonances.

The reaction of the FLP 4 with the conjugated enyne 12 took a similar course (Scheme 3) and we isolated the respective zwitterionic phosphonium/enynyl borate product 13 in 55% yield. It shows similar spectroscopic features as its congener 11 [13, for example,  $^{11}\text{B}$  NMR:  $\delta = -16.6 \text{ ppm}$ ,  $^{31}\text{P}$  NMR:  $\delta = -0.4 \text{ ppm}$  ( $J_{\text{PH}} \approx 468 \text{ Hz}$ )] and we observed the typical  $^1\text{H}$  NMR signals of the  $-\text{C}\equiv\text{C}-\text{C}(\text{CH}_3)=\text{CH}_2$  group at boron (for details see the Supporting Information).

### Addition reactions to carbonyl compounds

The P/B FLP 4 undergoes 1,2-addition to benzaldehyde.<sup>[20]</sup> We performed the reaction at room temperature in pentane and isolated the product as a solid mixture of two isomers 15a/15b in a ratio of ca. 62:38 (in  $\text{CD}_2\text{Cl}_2$ ) (Scheme 4). Both isomers showed the same principal relative atom connectivity with the nucleophilic carbonyl oxygen having become connected to boron and the electrophilic carbonyl carbon atom to phosphorus. The system 15 contains three stereogenic carbon atoms: two at the five-membered ring, the stereochemistry of which is dependent on each other as a result of their formation by the hydroboration reaction, and the newly formed stereogenic center derived from the binding of the former aldehyde reagent. From the X-ray crystal structure analysis (Figure 4) and a series of NOE experiments we assigned the major diastereoisomer 15a the *rac*-(*R, R, R*) configuration; that is, the C–H vectors at C6 and C2 inside the newly formed heterocyclic six-membered ring are in a *cis*-arrangement. Actually we noticed a dynamic behavior of the 15a/b pair in the NOE experiments,

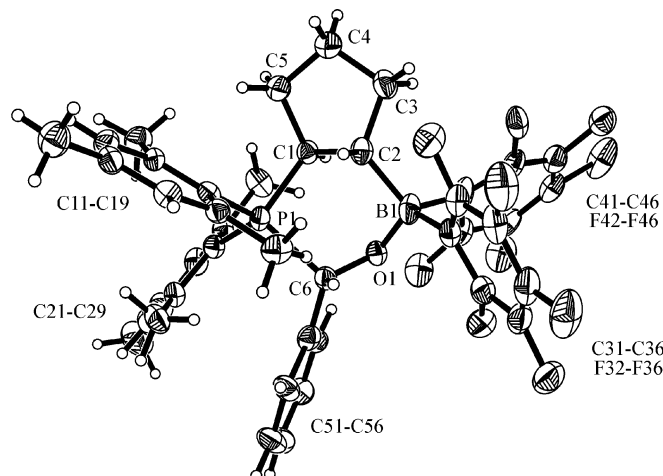


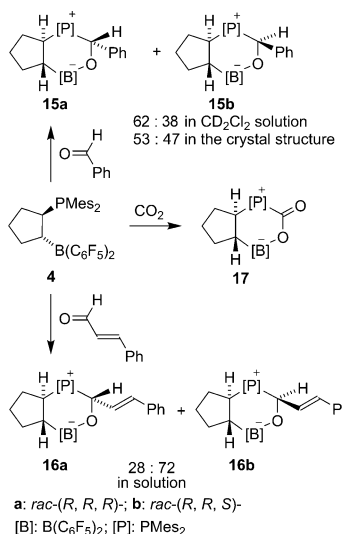
**Figure 4.** A view of the major isomer *rac*-*R, R, R* 15a from the addition reaction of benzaldehyde to FLP 4 (ellipsoids are set at 30% probability). Selected bond lengths [ $\text{\AA}$ ] and angles [ $^\circ$ ]: P1–C1: 1.822(4), C1–C2: 1.570(4), C2–B1: 1.639(6), B1–O1: 1.452(6), O1–C6: 1.388(9), P1–C6: 1.970(7), C6–C51: 1.513(11), C1–P1–C6: 98.0(2), C21–P1–C11: 109.9(5), O1–B1–C2: 106.1(3), C31–B1–C41: 105.3(3), P1–C1–C2–B1: 66.6(4), B1–O1–C6–P1: 83.4(7),  $\Sigma B^{CCC}$ : 333.9,  $\Sigma P^{C1C1C21}$ : 332.5.

namely irradiation at the  $\text{O}-\text{C}[\text{H}]-\text{P}$  (6-H) signal of the major isomer 15a gave a marked negative NOE response at the respective (6-H)  $^1\text{H}$  resonance of the minor isomer 15b. This indicates some  $15\text{a} \rightleftharpoons 15\text{b}$  rearrangement on the NMR timescale, a feature that had previously been observed of other benzaldehyde P/B FLP addition products as well.<sup>[21]</sup>

The X-ray crystal structure analysis confirmed the formation of the heterocyclic core of the product by B–O and P–C bond formation of FLP 4 to the incoming benzaldehyde moiety. In the crystal we found two diastereoisomers, the major isomer *rac*-*R, R, R* 15a (53%) and the minor isomer *rac*-*R<sup>C1</sup>, R<sup>C2</sup>, S<sup>C6</sup> 15b (47%). The core heterobicyclo[4.3.0]nonane framework of compound 15 shows a *trans*-junction between the two rings (Figure 4).*

The NMR spectra of the system 15 show mostly well-separated signals of the major (15a) and minor (15b) isomer. At 273 K both the rotation around the P–C(Mes) as well as the B–C( $\text{C}_6\text{F}_5$ ) vectors are frozen on the NMR timescale. Consequently, we observed a total of 6 mesityl  $\text{CH}_3$   $^1\text{H}$  NMR signals for each isomer and pairs of *o*-, *p*-, *m*- $^{19}\text{F}$  signals of the  $\text{C}_6\text{F}_5$  groups. The  $^1\text{H}$  NMR resonances of the  $\text{O}-\text{CH}[\text{P}]$  protons were located at  $\delta = 6.41 \text{ ppm}$  (major isomer 15a) and  $\delta = 5.89 \text{ ppm}$  (minor isomer 15b), respectively, and we find two  $^{31}\text{P}$  NMR resonances:  $\delta = 43.2 \text{ ppm}$  (15a),  $\delta = 28.5 \text{ ppm}$  (15b).

The FLP addition reaction to *trans*-cinnamic aldehyde proceeds similarly (Scheme 4). We isolated a circa 28:72 mixture of the respective 1,2-carbonyl addition products 16a and 16b from the pentane reaction mixture as a colorless solid in 62% yield. The detailed NMR/X-ray diffraction analysis showed that in this case the *rac*-*R<sup>C1</sup>, R<sup>C2</sup>, S<sup>C6</sup> diastereoisomer 16b was the major product. It features the 6-H and 2-H protons in a *trans*-arrangement. The ring junction is again *trans* (for details see the Supporting Information).*



**Scheme 4.** Reactions of the P/B FLP **4** with carbonyl compounds.

The *trans*-P/B FLP **4** reacts readily with carbon dioxide.<sup>[22,23]</sup> We exposed a solution of **4** in pentane to a CO<sub>2</sub> atmosphere at room temperature. Reaction overnight furnished a precipitate of the addition product **17** (Scheme 4), which was isolated as a colorless solid in 80% yield. This CO<sub>2</sub>/FLP adduct is remarkably stable. Its thermal stability is somewhere intermediate between typical intra- and intermolecular FLP-CO<sub>2</sub> adducts.<sup>[22a]</sup> It can even be handled for short periods of time at room temperature, but we measured the NMR spectra conveniently at lower temperatures to avoid any decomposition by CO<sub>2</sub> elimination altogether. Compound **17** was characterized by C, H elemental analysis, by spectroscopy, and by X-ray diffraction (Figure 5).

Single crystals of compound **17** were obtained by the diffusion method. The X-ray crystal structure analysis shows that

the P/B FLP has 1,2-added to one carbonyl group of carbon dioxide. The resulting heterobicyclic framework of compound 17 shows a *trans*-junction between the two rings ( $\theta$  B1-C2-C1-P1: 69.0(3°). Both the boron and the phosphorus atoms show pseudo-tetrahedral coordination geometries ( $\Sigma$ B1<sup>CCC</sup>: 336.8°,  $\Sigma$ P1<sup>C1C6C11</sup>: 326.0°). The carbon atom C6 is planar-tricoordinate ( $\Sigma$ C6<sup>OOP</sup>: 359.9°).

In solution, compound **17** features the  $^{13}\text{C}$  NMR carbonyl carbon atom signal at  $\delta=160.9$  ppm ( $^1\text{J}_{\text{PC}}=87.9$  Hz) and a  $^{31}\text{P}$  NMR resonance at  $\delta=11.3$  ppm. Compound **17** shows hindered rotation around the B–C( $\text{C}_6\text{F}_5$ ) and the P–C(Mes) vectors at low temperature leading to the observation of five (two overlapping)  $^1\text{H}$  mesityl methyl NMR signals plus four mesityl methine signals as well as four *o*- $\text{C}_6\text{F}_5$ , two *p*- and four *m*- $\text{C}_6\text{F}_5$   $^{19}\text{F}$  NMR resonances. Compound **17** shows an IR carbonyl stretching band at  $\tilde{\nu}=1699\text{ cm}^{-1}$ .

## 1.1-Addition reactions of the P/B FLP 4

1,1-Addition to a variety of reagents is a typical reaction feature of some vicinal P/B FLPs. Compound **4** shows a similar behavior towards some of those reagents. P/B Lewis pairs can undergo 1,3-, 1,2-, or even 1,1-addition reactions to organic aryl azides.<sup>[20,24]</sup> Some of the resulting products can be viewed as internally Lewis acid trapped intermediates of the Staudinger reaction.<sup>[25]</sup> Some such systems actually lose dinitrogen upon heating and yield Staudinger reaction type products, but a few undergo an anomalous Staudinger reaction.<sup>[26]</sup>

The reactive P/B FLP **4** rapidly undergoes a 1,1-addition reaction to the terminal azide nitrogen atom of mesityl azide ( $N_3$ -Mes) (Scheme 5). The product **18** was isolated in 78% yield. The X-ray crystal structure analysis (Figure 6) shows the newly formed geminal pair of N–B and N–P bonds at the azide nitrogen atom N1. The resulting heterobicyclic framework again shows a *trans*-junction. The remaining  $-N=N-$ Mes substituent shows a *trans*-nitrogen–nitrogen double bond.

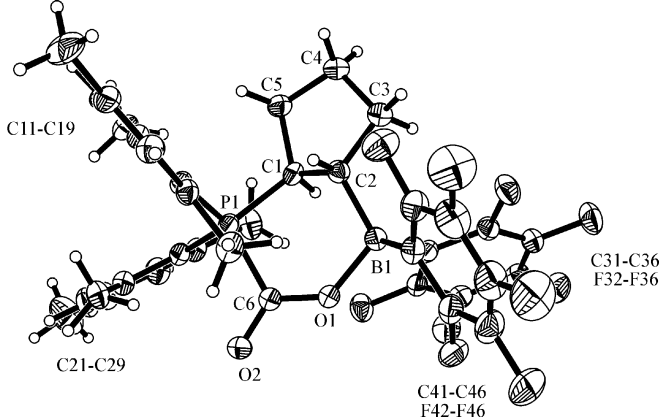
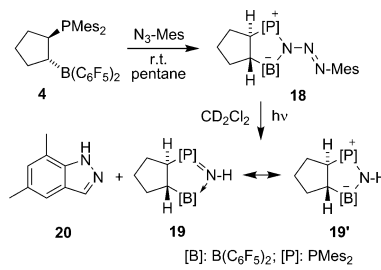


**Figure 5.** Molecular structure of the P/B FLP CO<sub>2</sub> addition product **17** (only molecule A of two independent molecules is shown; ellipsoids are set at 30% probability). Selected lengths [Å] and angles [°]: P1—C1: 1.817(3), C1—C2: 1.547(4), C2—B1: 1.623(4), B1—O1: 1.548(4), O1—C6: 1.287(4), O2—C6: 1.209(4), P1—C6: 1.900(3), C1—P1—C6: 102.2(1), C21—P1—C11: 110.5(1), O1—B1—C2: 111.3(3), C41—B1—C31: 108.4(3), O1—C6—P1: 119.6(2), O2—C6—P1: 115.8(2), O2—C6—O1: 124.5(3), P1—C1—B1: 69.0(3), B1—O1—C6—P1: 2.5(4),  $\Sigma B^{CCC}$ : 336.8,  $\Sigma PC^{CCG}$ : 326.0,  $\Sigma C6^{OOP}$ : 359.9.



**Scheme 5.** Reactions of the P/B FLP 4 with mesityl azide.

The periphery of compound **18** is congested. This led to the observation of hindered rotation around the heteroatom-C(aryl) bonds and thus we observed a total of ten  $^{19}\text{F}$  NMR  $\text{C}_6\text{F}_5$  resonances and six  $^1\text{H}$  NMR methyl signals plus four aromatic methine resonances of the endocyclic  $\text{PMes}_2$  groups. In contrast, the peripheral  $-\text{N}=\text{N}-\text{mesityl}$  substituent shows only three  $^1\text{H}$  NMR signals (arom. CH, *p*-CH<sub>3</sub>, *o*-CH<sub>3</sub>) in a 2:3:6 intensity ratio.

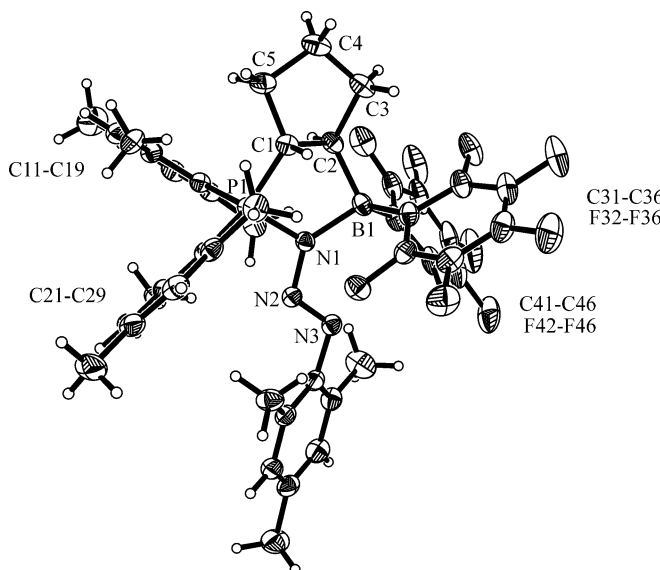


**Figure 6.** A view of the 1,1-addition product **18** of the P/B FLP **4** to mesityl azide (ellipsoids are set at 30% probability). Selected bond lengths [Å] and angles [°]: P1–C1: 1.809(2), C1–C2: 1.554(3), C2–B1: 1.629(4), P1–N1: 1.676(2), B1–N1: 1.629(3), N1–N2: 1.386(3), N2–N3: 1.246(3), N3–C51: 1.439(3), N1–P1–C1: 93.5(1), C11–P1–C21: 107.1(1), N1–B1–C2: 96.6(2), C41–B1–C31: 106.7(2), B1–N1–P1: 116.2(2), N2–N1–P1: 109.8(1), N2–N1–B1: 134.1(2), P1–C1–C2–B1: −54.0(2),  $\Sigma B^{CC}$ : 334.7,  $\Sigma P^{CC}$ : 335.5,  $\Sigma N1^{PNB}$ : 360.0.

Upon photolysis (HPK 125) in  $\text{CH}_2\text{Cl}_2$ , compound **18** undergoes an anomalous Staudinger reaction<sup>[24,26]</sup> with formation of the indazole derivative **20** (identified from the reaction mixture by NMR and comparison with the data of the known compound) and the phosphinimine/borane adduct **19**. Compound **19** was isolated from the reaction mixture by column chromatography.

The X-ray crystal structure analysis shows the presence of the endocyclic  $[\text{P}]=\text{N}-\text{H}$  phosphinimine moiety (Figure 7). Consequently, the P1–N1 bond of **19** is rather short (1.622(1) Å), which is shorter than the corresponding P1–N1 bond of its

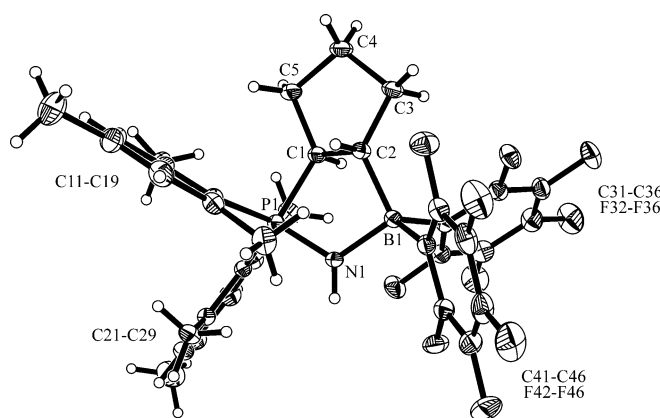
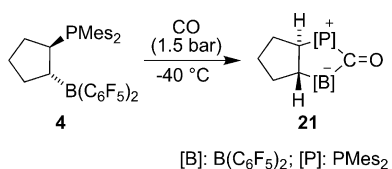


**Figure 7.** Molecular structure of the product **19** of an anomalous Staudinger reaction (ellipsoids are set at 30% probability). Selected bond lengths [Å] and angles [°]: P1–C1: 1.809(2), C1–C2: 1.563(2), C2–B1: 1.630(2), P1–N1: 1.622(1), N1–B1: 1.581(2), N1–P1–C1: 95.1(1), C21–P1–C11: 107.4(1), N1–B1–C2: 99.1(1), C31–B1–C41: 107.0(1), B1–N1–P1: 115.8(1), P1–C1–C2–B1: 51.6(1),  $\Sigma B^{CC}$ : 336.1,  $\Sigma P^{CC}$ : 335.5.

precursor **18** (1.676(2) Å), but due to its internal borane Lewis acid coordination it is longer than typical phosphinimine  $\text{P}=\text{N}$ -bonds ( $\text{Ph}_3\text{P}=\text{NH}$  1.524(3) Å).<sup>[27]</sup> The B1–N1 bond in **19** is also rather short at 1.581(2) Å; both these values indicate a delocalized structure as described by the mesomeric formulae **19**↔**19** in Scheme 5.

Vicinal P/B Lewis pairs contain a phosphorus donor and a boron acceptor center. Some such systems have been used as ambiphilic ligands for metal complex coordination,<sup>[28]</sup> but P/B Lewis pairs can apparently also undergo synergistic donor/acceptor bonding,<sup>[29]</sup> with for example CO, in a way that is itself reminiscent of metal coordination.<sup>[30]</sup>

Compound **4** reacted with carbon monoxide in dichloromethane/pentane solution at 2 bar CO pressure at temperatures below  $-40^\circ\text{C}$  to give the cooperative P/B FLP addition product **21** (Scheme 6). Crystallization gave the cyclic carbonyl in 52% yield.



**Scheme 6.** 1,1-P/B addition reaction of FLP **4** to CO.

The X-ray crystal structure analysis showed that both the boron Lewis acid and the phosphorus Lewis base had added to the carbonyl carbon of CO. The carbonyl carbon atom is planar-tricoordinate ( $\Sigma C_6^{POB} = 360.0^\circ$ ) and the C6–O1 linkage is short. The C=O group is somewhat leaning over toward phosphorus as if the phosphorus Lewis base had trapped a borane carbonyl (Figure 8). The P1/B1 separation in compound **21** is 2.99 Å.

Compound **21** was also characterized by magic angle spinning solid-state NMR spectroscopy (Figure 9; see the Supporting Information for details).<sup>[31]</sup> Consistent with the fourfold boron coordination, the  $^{11}\text{B}$  MAS-NMR spectrum reveals a rather small quadrupolar coupling constant of 0.85 MHz. The  $^{31}\text{P}$  MAS-NMR lineshape is not influenced by  $^{11}\text{B}$ – $^{31}\text{P}$  spin–spin coupling even though  $^2J(^{11}\text{B}; ^{31}\text{P})$  amounts to 55 Hz as determined by heteronuclear *J*-resolved spectroscopy (for details see the Supporting Information). The NMR observables measured on compound **21** are found to be in excellent agreement with the values calculated by quantum chemical methods on DFT level. Finally, Figure 9 (top) shows the experimentally observed  $^{11}\text{B}$ { $^{31}\text{P}$ } rotational echo double resonance (REDOR) curve of **21**. Based on simulations of the oscillatory behavior measured at long dipolar mixing times, the  $^{11}\text{B}$ – $^{31}\text{P}$  internuclear distance is measured as  $305 \pm 5$  pm, which is found to be in excellent agreement with the crystal structure. These results demonstrate the ability of REDOR to characterize the weaker  $^{11}\text{B}$ – $^{31}\text{P}$  dipole–dipole couplings of FLP adducts, which generally occur over longer distance ranges.

Compound **21** shows a typical IR feature at  $\tilde{\nu} = 1774 \text{ cm}^{-1}$ . The solution-state  $^{13}\text{C}$  NMR C=O resonance of **21** was located

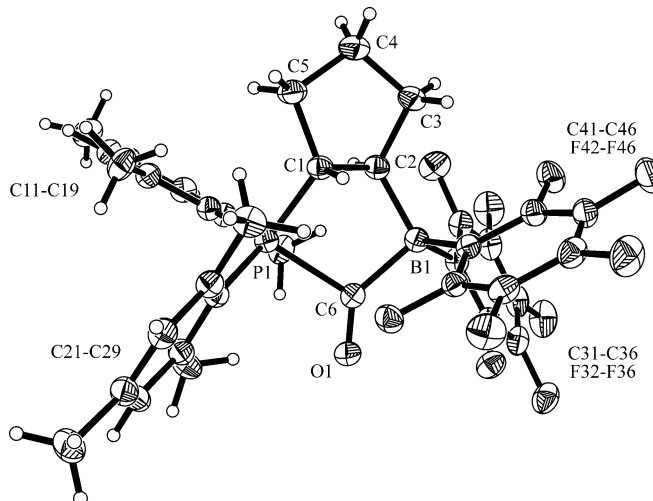


**Figure 8.** A view of the molecular structure of the cooperative P/B FLP CO addition product **21** (ellipsoids are set at 30 % probability). Selected bond lengths [Å] and angles [°]: P1–C1: 1.820(2), C1–C2: 1.557(2), C2–B1: 1.630(2), P1–C6: 2.071(2), C6–B1: 1.670(2), O1–C6: 1.181(2), C1–P1–C6: 90.8(1), C21–P1–C11: 108.5(1), C2–B1–C6: 102.2(1), C41–B1–C31: 109.7(1), B1–C6–P1: 105.8(1), O1–C6–P1: 119.4(1), O1–C6–B1: 134.9(2), P1–C1–C2–B1: -59.4(1),  $\Sigma C_6^{BOP}$ : 360.0,  $\Sigma B^{C_2C_3C_4}$ : 339.0,  $\Sigma P^{C_1C_1C_2}$ : 336.7.

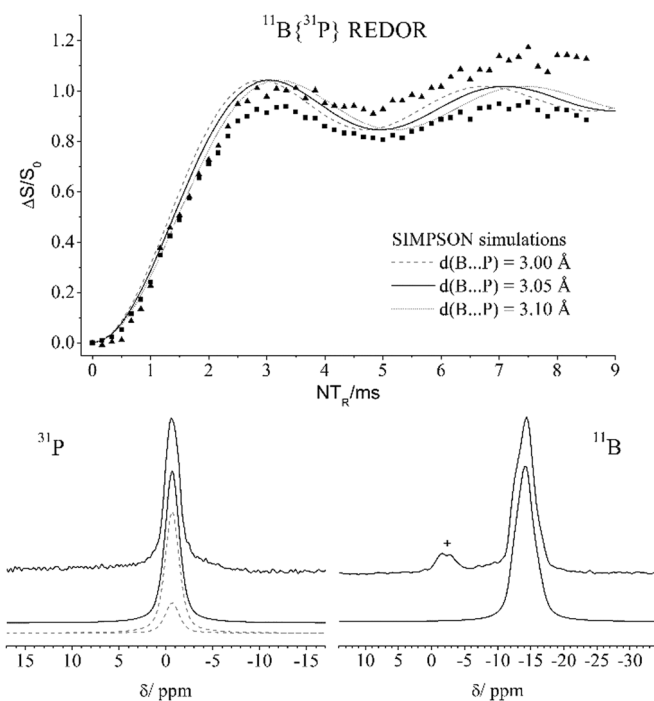
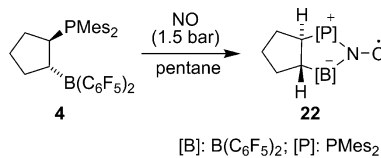


**Figure 9.** Top:  $^{11}\text{B}\{^{31}\text{P}\}$  REDOR data of **21**: Squares show uncorrected experimental data, while triangles show corrected data obtained with a compensated REDOR method.<sup>[32]</sup> Simulations for three different B···P distances are shown; the best agreement with the experimental data is found for a B···P distance of 305 pm. Bottom:  $^{11}\text{B}$  (right) and  $^{31}\text{P}$  (left) MAS-NMR spectra of compound **21**. Upper traces show experimental data and lower traces are simulated spectra. An impurity is marked by the symbol +.

at  $\delta = 229.8$  ppm; it shows a large  $J_{\text{PC}}$  coupling constant of ca. 102 Hz. The  $^{31}\text{P}$  NMR resonance of **21** is at  $\delta = -0.8$  ppm and the  $^{11}\text{B}$  NMR signal at  $\delta = -12.2$  ppm. The  $\text{C}_6\text{F}_5$  substituents at

boron and the mesityl groups at phosphorus in **21** are diastereotopic and both show hindered rotation around the heteroatom–C(aryl) vectors on the NMR timescale at 223 K.

The FLP **4** was found to react rapidly with NO. We stirred a pale yellow solution of **4** in pentane at  $-78^\circ\text{C}$  under a NO atmosphere (2 bar). Within minutes a precipitate formed and the product **22** (Scheme 7) was isolated at room temperature as a pale turquoise crystalline solid in 83 % yield.



**Scheme 7.** Reactions of the P/B FLP **4** with nitric oxide.

Single crystals of the persistent P/B FLPNO nitroxide radical **22** were obtained from cyclopentane/dichloromethane by the diffusion method. The X-ray crystal structure analysis (Figure 10 and Table 1) showed that the NO molecule had been captured by forming a pair of B–N and P–N bonds. The resulting N–O bond is short ( $\leq 1.3$  Å), but markedly longer than the N–O distance in free NO (1.15 Å).<sup>[33]</sup> The nitrogen coordination in com-

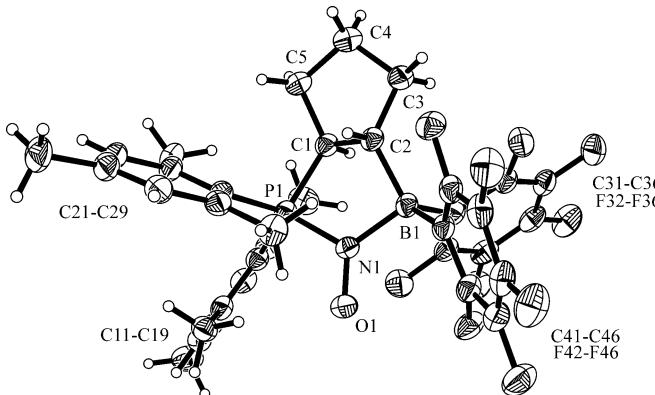


**Figure 10.** Molecular structure of the persistent P/B FLPNO nitroxide radical **22** (ellipsoids are set at 30 % probability). Selected bond lengths [Å] and angles [°]: P1–C1: 1.806(4), C1–C2: 1.559(5), C2–B1: 1.626(6), P1–N1: 1.716(3), B1–N1: 1.604(5), O1–N1: 1.299(4), N1–P1–C1: 93.0(2), C11–P1–C21: 107.2(2), N1–B1–C2: 97.6(3), C41–B1–C31: 108.7(3), B1–N1–P1: 115.9(2), P1–C1–C2–B1: 52.4(3),  $\Sigma B^{CCC}$ : 339.9,  $\Sigma P^{CCC}$ : 338.6.

**Table 1.** Selected structural parameters of the compounds **22–24**<sup>[a]</sup>

[N]OX	<b>22</b> [N]O	<b>23</b> [N]OH	<b>24</b> [N]OCH <sub>2</sub> Ph
N1–O1	1.299(4)	1.432(3)	1.436(2)
P1–N1	1.716(3)	1.635(3)	1.647(2)
B1–N1	1.604(5)	1.553(4)	1.593(3)
B1–N1–O1	125.7(3)	123.2(2)	123.4(2)
P1–N1–O1	118.4(2)	117.4(2)	116.0(1)
$\Sigma N^{BOP}$	360.0	360.0	356.9
P1–C1–C2–B1	52.4(3)	-51.1(3)	-52.6(2)

ponent **22** is trigonal planar, although the individual bond angles around nitrogen are quite different from each other. It again appears that the N–O unit is slightly leaning over toward phosphorus (Table 1), similar to the way it had been observed for the CO addition product **21**.<sup>[34]</sup>

The FLPNO radical **22** was characterized by EPR spectroscopy in solution. It shows a multi-line pattern in dichloromethane at room temperature (Figure 11). The spectrum is centered at  $g=2.00644$  and exhibits coupling to  $^{31}\text{P}$  [ $A(^{31}\text{P})=50.8$  MHz],  $^{14}\text{N}$  [ $A(^{14}\text{N})=22.0$  MHz], and  $^{11}\text{B}/^{10}\text{B}$  [ $A(^{11}\text{B})=9.2$  MHz]. A detailed discussion of the solid-state EPR spectrum of compound **22** has been recently published separately.<sup>[35]</sup>

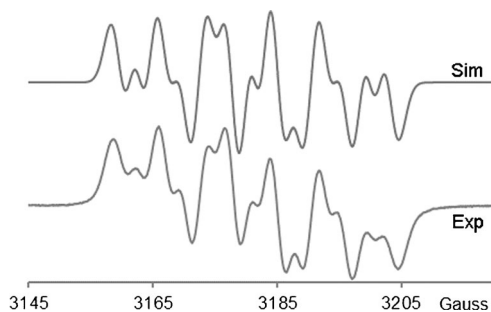


**Figure 11.** X-band EPR spectrum (bottom) and simulation (top) of compound **22** in dichloromethane at room temperature.

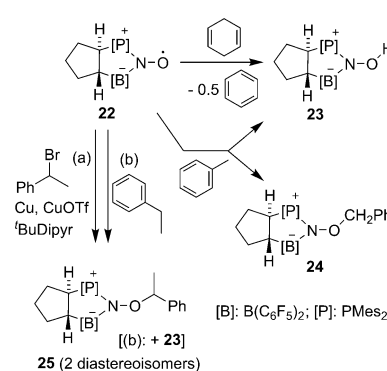
Compound **22** is a markedly oxygen-centered nitroxide radical. It undergoes the typical reactions of the general class of compounds of the nitroxide radical type.<sup>[36]</sup> The P/B FLPNO radical **22** undergoes H-atom abstraction reactions (Scheme 8). With 1,4-cyclohexadiene it reacts at room temperature in dichloromethane to give the diamagnetic P/B FLPNOH product **23** (plus benzene). Compound **23** was characterized by X-ray diffraction (the structure is depicted in the Supporting Information). The structural parameters show that the H<sup>+</sup> addition to give the [N]–O–H product resulted in a marked lengthening of the N–O bond (Table 1). Compared to the radical **22**, the N–O[H] bond in **23** is 0.133 Å longer. At the same time the P–N bond has become shorter by 0.081 Å, which probably indicates some phosphinimine character of **23**.

The P/B FLPNOH product **23** shows an IR O–H band at  $\tilde{\nu}=3531\text{ cm}^{-1}$ . In solution it features heteronuclear magnetic resonance signals at  $\delta=+46.3$  ppm ( $^{31}\text{P}$ ) and  $\delta=-5.7$  ppm ( $^{11}\text{B}$ ), respectively. The  $^1\text{H}$  NMR [N]OH resonance occurs as a multiplet at  $\delta=4.83$  ppm. Compound **27** shows the signals of pairwise diastereotopic  $C_6\text{F}_5$  groups at boron ( $^{19}\text{F}$ ) and mesityl groups at phosphorus ( $^1\text{H}$ ). There is hindered rotation around the B–C(aryl) and P–C(aryl)  $\sigma$ -bonds on the NMR timescale at 299 K.

The P/B FLPNO radical **22** activates a benzylic hydrogen of toluene. At 60 °C the H-atom abstraction gives a mixture of the P/B FLPNOH (**23**) and P/B FLPNO-benzyl (**24**) products. The reaction is thought to be initiated by hydrogen atom abstraction from toluene by **22** generating **23** and a very reactive benzyl radical which is instantaneously trapped by additional nitroxide radical **22** to give **24**. Compound **24** was also characterized by

X-ray diffraction and by spectroscopy (for details, see the Supporting Information).

The analogous reaction of **22** was carried out with ethylbenzene to give a ca. 1:1 mixture of the diastereoisomers of **25** (Scheme 8). Unfortunately we could isolate this product only in very low yield (3%). Therefore, we prepared **25** according to a Matyjaszewski method<sup>[37]</sup> by treatment of **22** with phenylethylbromide and Cu/CuOTf in the presence of a substituted dipyridyl ligand. This eventually gave the **25a/25b** mixture of diastereoisomers in a combined yield of 38%. One of the isomers could be crystallized and characterized by X-ray diffraction (the structure is depicted in the Supporting Information, see there also for the spectroscopic characterization of the compounds).



**Scheme 8.** Some typical reactions of the persistent P/B FLPNO-radical **22**.

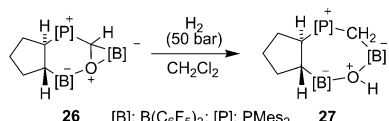
The P/B FLPNO-CHMePh products **25a/25b** were tested to serve as initiators/regulators in the nitroxide mediated (radical) polymerization (NMP) of styrene.<sup>[38]</sup> Experiments were conducted with 0.5 mol % of **25a/25b** in neat styrene at 110–150 °C for 1–5 h in the presence of varying amounts of additional free nitroxide **22** (for details, see the Supporting Information). Under the tested conditions controlled styrene polymerization was not achieved, as revealed by PDIs significantly above the theoretical limit of 1.5 (1.59–1.81). For example, at 120 °C after 3 h, poly(styrene) with an average molecular weight of  $M_n=23.9\text{ kDa}$  and a PDI of 1.59 was isolated after precipitation into methanol (30% yield).

We had recently studied the application of a structurally related FLP-derived alkoxyamine in the NMP of styrene.<sup>[34b]</sup> Unlike **25a/25b**, the former system features a cyclohexane instead of a cyclopentane ring annulated with the cyclic FLP-alkoxyamine in its backbone. Under similar conditions, good control of the polymerization was obtained with that homologue, and poly(styrene) with PDIs between 1.30 and 1.35 had been isolated. Obviously, the ring size of the second ring in these bicyclic P/B FLPs influences the effectiveness of the FLPNO radicals in controlling the radical polymerization reaction.

#### Carbon monoxide reactions and formylborane chemistry

We had previously shown that carbon monoxide can be reduced to the formyl stage by BH boranes at suited FLP tem-

plates. The FLP template serves to overcome the thermodynamic restrictions of CO reduction by [B]-H boranes.<sup>[39]</sup> In this way we had prepared the FLP **4** generated *in situ*.<sup>[13]</sup> We now treated the product **26** with H<sub>2</sub> (50 bar, 30 h). This resulted in a further reduction of the carbon monoxide derived formyl group with cleavage of the strong C–O bond to the methylene stage (Scheme 9).<sup>[40]</sup> Product **27** was eventually isolated as a colorless crystalline solid in 51% yield.



**Scheme 9.** Reaction of the ( $\eta^2$ -formylborane) FLP product **26** with dihydrogen.

The X-ray crystal structure analysis shows the newly formed CH<sub>2</sub> group bridging between phosphorus and boron and the separated former carbonyl oxygen atom protonated bridging between the pair of boron atoms (Figure 12). The B1-O1-B2 angle at this unit amounts to 129.1(2) $^\circ$ .

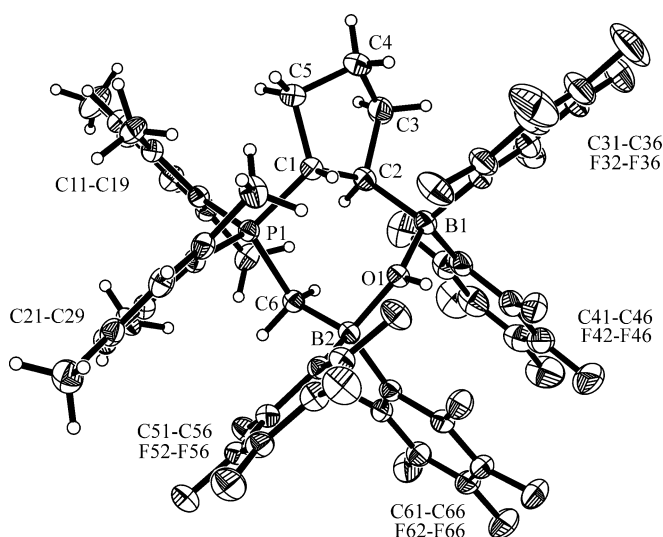
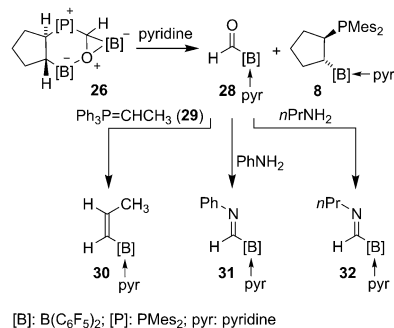


**Figure 12.** A view of the molecular structure of the CO-reduction product **27** (ellipsoids are set at 30% probability). Selected bond lengths [ $\text{\AA}$ ] and angles [ $^\circ$ ]: P1–C1: 1.841(2), C1–C2: 1.573(3), C2–B1: 1.636(3), P1–C6: 1.807(2), C6–B2: 1.635(3), O1–B1: 1.600(3), O1–B2: 1.553(3), C6–P1–C1: 104.7(1), C21–P1–C11: 108.4(1), B2–C6–P1: 118.8(1), O1–B2–C6: 106.2(2), C61–B2–C51: 105.7(2), B2–O1–B1: 129.1(2), O1–B2–C2: 107.6(2), C31–B1–C41: 109.7(2), P1–C1–C2–B1: -96.7(2),  $\Sigma$ B1<sup>CCC</sup>: 337.0,  $\Sigma$ B2<sup>CCC</sup>: 331.9,  $\Sigma$ P1<sup>C1C1C21</sup>: 333.5.

The <sup>19</sup>F NMR spectrum of compound **27** in CD<sub>2</sub>Cl<sub>2</sub> solution shows the signals of four different C<sub>6</sub>F<sub>5</sub> substituents at the pair of boron atoms. The compound features diastereotopic mesityl groups at phosphorus that show hindered rotation on the NMR timescale, giving rise to six <sup>1</sup>H NMR methyl signals and four aromatic CH groups. Compound **27** shows two <sup>11</sup>B NMR

resonances ( $\delta=4.3$  and  $\delta=0.7$  ppm) and a <sup>31</sup>P NMR signal at  $\delta=36.5$  ppm. The newly formed CH<sub>2</sub> group inside the seven-membered ring shows diastereotopic hydrogen atoms ( $\delta=3.36$  and  $\delta=2.76$  ppm) with coupling constants <sup>2</sup>J<sub>PH</sub>=<sup>2</sup>J<sub>HH</sub>=14.5 Hz. We observe a resonance of relative intensity one at  $\delta=5.78$  ppm that was assigned to the OH proton; it appears as a doublet due to coupling with a fluorine atom of one of the adjacent C<sub>6</sub>F<sub>5</sub> groups ( $J_{FH}=12.2$  Hz, shown by a selective decoupling experiment).<sup>[41]</sup>

We had previously shown that FLP- $\eta^2$ -formylborane systems can react in two different ways with pyridines depending on the specific FLP framework. They can either undergo a nucleophilic aromatic formyl transfer to the pyridine framework, a reaction that eventually yields a hydroxymethylation product,<sup>[42]</sup> or liberate the genuine formylborane as the pyridine adduct.<sup>[40,43]</sup> The latter reaction is favored with the FLP- $\eta^2$ -formylborane **26**. The reaction of **26** with excess pyridine in dichloromethane (3 h, room temperature) gave a ca. 1:1 mixture of the pyridine-stabilized formylborane **28** and the FLP pyridine adduct **8** (Scheme 10). Crystallization from toluene/n-pen-



**Scheme 10.** Formation and carbonyl reactions of the pyridine stabilized formylborane **28**.

tane then gave the pure pyridine formylborane product **28** in 67% yield [[B]–CHO:  $\delta=11.24$  (<sup>1</sup>H),  $\delta=233.2$  (<sup>13</sup>C),  $\delta=-4.5$  ppm (<sup>11</sup>B)]. It undergoes a variety of typical organic carbonyl reactions. The Wittig olefination reaction with Ph<sub>3</sub>P=CHCH<sub>3</sub> (**29**) gave the substituted vinylborane **30** (Scheme 10), isolated as a viscous oil in 48% yield [<sup>1</sup>H NMR:  $\delta=6.16$ , 6.08 ppm, <sup>3</sup>J<sub>HH</sub>=13.5 Hz, <sup>13</sup>C NMR:  $\delta=138.4$ , 135.1 ppm ( $-\text{CH}=\text{CH}-$ ),  $\delta=17.2$  (CH<sub>3</sub>), <sup>11</sup>B NMR:  $\delta=-3.6$  ppm].<sup>[40]</sup>

Reaction of the formylborane **28** with aniline (dichloromethane, 2 d, room temperature) gave the aldimine **31** (Scheme 10), isolated as a crystalline solid in 54% yield. The X-ray crystal structure analysis shows the presence of a *trans*-configured imine C=N double bond with a trigonal-planar carbonyl carbon atom C1. The boron atom shows a pseudo-tetrahedral coordination sphere. It contains the stabilizing pyridine ligand as an essential structural element (Figure 13).

Compound **31** shows a <sup>1</sup>H NMR –CH=N– carbaldimine resonance at  $\delta=8.79$  ppm ( $\delta^{13}\text{C}$ : 182.5 ppm) and a <sup>11</sup>B NMR signal at  $\delta=-3.7$  ppm. The IR  $\tilde{\nu}$ (C=N) stretching band of **31** was located at  $\tilde{\nu}=1647\text{ cm}^{-1}$ . The analogous reaction of compound **28** with *n*-propyl amine gave the borane carbaldimine product

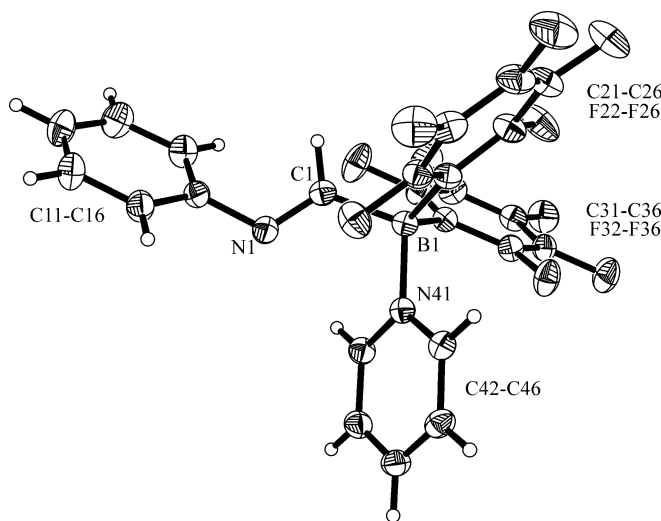


**Figure 13.** Molecular structure of the pyridine stabilized borane formaldimine **31** (ellipsoids are set at 30 % probability). Selected bond lengths [Å] and angles [°]: B1–C1: 1.614(3), B1–N41: 1.616(3), C1–N1: 1.265(3), N1–C11: 1.421(3), C1–B1–N41: 108.8(2), C31–B1–C21: 114.3(2), N1–C1–B1: 125.5(2), C1–N1–C11: 118.7(2), C11–N1–C1–B1: 178.1(2),  $\Sigma$ B1<sup>ccc</sup>: 333.0.

**32** (Scheme 10), isolated as a colorless solid in 63 % yield [IR:  $\tilde{\nu}$  = 1644 cm<sup>-1</sup>; <sup>1</sup>H/<sup>13</sup>C NMR:  $\delta$  = 8.55/180.0 ppm ( $-\text{CH}=\text{N}-$ ), <sup>11</sup>B NMR:  $\delta$  = -4.1 ppm].

## Conclusion

Intramolecular vicinal FLPs have considerably contributed to the development of frustrated Lewis pair chemistry.<sup>[9–11]</sup> Many such systems exhibit some internal Lewis acid–base interaction, although it is thought that their typical reactions with small molecules take place from energetically higher-lying open isomers, reached in an endergonic equilibrium situation. Therefore, it was an attractive concept to develop vicinal frustrated Lewis pair systems that are devoid of such an intramolecular interaction. This can either be achieved by introducing extreme steric bulk<sup>[10b]</sup> or by placing the Lewis acid and Lewis base functionalities at specifically designed rigid frameworks that serve to effectively separate the protagonists from each other spatially. The norbornane derived FLP **3** is an example.

In this study we have shown that attaching the  $\text{B}(\text{C}_6\text{F}_5)_2$  and  $\text{PMes}_2$  functionalities in a trans-1,2-fashion at the cyclopentane backbone provides a solution to this problem. In contrast to cyclohexane-derived *trans*-P/B or N/B FLPs, which show internal interaction between the pair of equatorially oriented Lewis acid and Lewis base functions,<sup>[44]</sup> the corresponding cyclopentane derived system **4** is a free, non-interacting P/B FLP. Consequently, this is a reactive FLP which can undergo a variety of reactions that may be typical for either intra- or intermolecular FLPs. Some of the products show some interesting follow-up chemistry. It seems that the typical properties of the open P/B FLP **4** direct us toward an expansion of FLP structures and reactivities by using strictly non-interacting Lewis acid–base functionalities at suitably devised frameworks.

## Experimental Section

For general information and details of the characterization of the compounds, see the Supporting Information. Synthetic procedures for the preparation of selected examples are given below.

**4:** Equivalent amounts of dimesitylcyclopentenylphosphane (**5**) (100 mg, 0.297 mmol) and bis(pentafluorophenyl)borane (103 mg, 0.297 mmol) were dissolved in *n*-pentane (ca. 4 mL) and stirred at r.t. for ca. 10 min. The bright yellow solution was stored at -40 °C and after several weeks at -40 °C a yellowish crystalline solid was formed (140 mg, 0.205 mmol, 69%, compound **4**). The obtained crystals were suitable for the X-ray crystal structure analysis. Elemental analysis calcd for  $\text{C}_{35}\text{H}_{30}\text{BF}_{10}\text{P}$ : C 61.60, H 4.43; found: C 61.59, H 4.49.

## Reactions with dihydrogen

**7:** Compound **4** was prepared *in situ* by dissolving equivalent amounts of dimesitylcyclopentenylphosphane (**5**) (60.1 mg, 0.179 mmol) and bis(pentafluorophenyl)borane (61.9 mg, 0.179 mmol) in *n*-pentane (3 mL) and stirring at r.t. for ca. 10 min. The solution was degassed and  $\text{H}_2$  gas (2 bar) pressure was applied for a few minutes at r.t. The reaction mixture was stirred overnight upon which a white precipitate had formed. The solvent was removed by cannula filtration and the residue was washed with *n*-pentane (2 × 2 mL) and was dried in vacuo. The phosphonium hydridoborate **7** was obtained as a white powder (83.4 mg, 0.122 mmol, 68%). Elemental analysis calcd for  $\text{C}_{35}\text{H}_{32}\text{BF}_{10}\text{P}$ : C 61.42, H 4.71; found: C 61.68, H 5.02.

## Reactions with a terminal alkyne

**11:** Compound **4** was prepared *in situ* by dissolving equivalent amounts of dimesitylcyclopentenylphosphane (**5**) (50.1 mg, 0.149 mmol) and bis(pentafluorophenyl)borane (51.5 mg, 0.149 mmol) in *n*-pentane (2.5 mL) and stirring at r.t. for ca. 5 min. Phenylacetylene (16.0 mg, 0.157 mmol, 1.05 equiv) dissolved in *n*-pentane (1 mL) was added to the yellow solution, upon which a white precipitate was formed. The solution was removed by filter cannula, the residue washed with *n*-pentane (1 × 2 mL), and it was dried in vacuo to give compound **11** as a white powder (103.1 mg, 0.131 mmol, 88%). Elemental analysis calcd for  $\text{C}_{43}\text{H}_{36}\text{BF}_{10}\text{P}$ : C 65.83, H 4.63; found: C 65.72, H 4.66.

## Reactions with carbonyl compounds

**15:** FLP **4** was prepared *in situ* by dissolving equivalent amounts of dimesitylcyclopentenylphosphane (**5**) (70.2 mg, 0.209 mmol) and bis(pentafluorophenyl)borane (72.3 mg, 0.209 mmol) in *n*-pentane (3.5 mL) and stirring at r.t. for ca. 5 min. Benzaldehyde (23.5 mg, 0.221 mmol, 1.05 equiv) dissolved in *n*-pentane (1 mL) was added to the yellow solution to give a colorless suspension. The supernatant was removed by filter cannula, and the residue dried in vacuo, to finally give a white powder (132.9 mg, 0.169 mmol, 81%). The solution of compound **15** in  $[\text{D}_2]\text{dichloromethane}$  showed a mixture of 2 diastereoisomers **15a**/**15b** in a ratio of 62:38 (<sup>31</sup>P, 273 K). Crystals of compounds **15a** and **15b** suitable for the X-ray crystal structure analysis were obtained by slow diffusion of *n*-pentane into a solution of the obtained white solid in  $\text{CH}_2\text{Cl}_2$  at -40 °C. The obtained crystal contains compounds **15a** and **15b** (ratio: 53:47). Elemental analysis calcd for  $\text{C}_{42}\text{H}_{36}\text{BF}_{10}\text{OP}$ : C 63.98, H 4.60; found: C 64.32, H 4.41.

**16:** FLP **4** was prepared *in situ* by dissolving equivalent amounts of phosphane **5** (70.0 mg, 0.208 mmol) and bis(pentafluorophenyl)-

borane (72.0 mg, 0.208 mmol) in *n*-pentane (3.5 mL) and stirring at r.t. for ca. 5 min. *trans*-Cinnamic aldehyde (26.2  $\mu$ L, 0.208 mmol) was added to the yellow solution, upon which a white precipitate was formed. The solution was removed by filter cannula, and the residue dried in vacuo. Compound **16** was obtained as white powder (103.9 mg, 0.128 mmol, 62%). NMR analysis of a solution of the white solid in  $[D_2]$ dichloromethane showed a mixture of 2 diastereoisomers **16a/b** in 1:2.5 ratio ( $^1$ H NMR). Crystals of compound **16b** suitable for the X-ray crystal structure analysis were obtained by slow diffusion of *n*-pentane into a solution of the obtained white solid in  $CH_2Cl_2$  at  $-40^\circ C$ . Elemental analysis calcd for  $C_{44}H_{38}BF_{10}OP$ : C 64.88, H 4.70; found: C 64.83, H 4.60.

**17:** FLP **4** was prepared in situ by dissolving equivalent amounts of phosphane **5** (50.1 mg, 0.149 mmol) and bis(pentafluorophenyl)borane (51.3 mg, 0.149 mmol) in *n*-pentane (3 mL) and stirring at r.t. for ca. 10 min. The solution was degassed, and  $CO_2$  gas (2 bar) pressed on it at r.t. for a few minutes. The reaction mixture was stirred overnight upon which a white precipitate had formed. The solvent was removed by syringe, the residue washed with *n*-pentane (2  $\times$  2 mL), and dried in vacuo. Product **17** was obtained as a white powder (86.6 mg, 0.119 mmol, 80%). Crystals suitable for the X-ray crystal structure analysis were obtained by slow diffusion of *n*-pentane into a concentrated solution of compound **17** in  $CH_2Cl_2$  at  $-40^\circ C$ . Elemental analysis calcd for  $C_{36}H_{30}BF_{10}O_2P\cdot0.5CH_2Cl_2$ : C 57.02, H 4.06; found: C 57.02, H 3.79.

### 1,1-Addition reactions

**18:** Compound **4** was prepared in situ by dissolving equivalent amounts of phosphane **5** (70.0 mg, 0.208 mmol) and bis(pentafluorophenyl)borane (72.0 mg, 0.208 mmol) in *n*-pentane (4 mL) and stirring at r.t. for ca. 5 min. Mesitylazide (33.8 mg, 210 mmol) dissolved in *n*-pentane was added to the yellow solution, upon which a white precipitate was formed. The solution was removed by filter cannula, and the residue was dried in vacuo to give compound **18** as a white powder (136.3 mg, 0.162, 78%). Crystals of compound **18** suitable for the X-ray crystal structure analysis were obtained by slow diffusion of *n*-pentane into a solution of compound **18** in  $CH_2Cl_2$  at  $-40^\circ C$ . Elemental analysis calcd for  $C_{44}H_{41}BF_{10}N_3P$ : C 62.65, H 4.90, N 4.98; found: C 63.08, H 4.80, N 5.01.

**19:** Compound **18** (40.0 mg, 0.0474 mmol) was dissolved in  $CH_2Cl_2$  (1.5 mL) and the solution submitted to UV irradiation for 90 h, after which it was converted into a 1:1 mixture of phosphinimine compound **19** and indazole derivative **20**. The compounds were separated by column chromatography, and crystallization from  $CH_2Cl_2$  gave pure compound **19** as off-white crystalline material (25.2 mg, 0.0361 mmol, 76%). The obtained crystals were suitable for the X-ray crystal structure analysis. Elemental analysis calcd for  $C_{35}H_{31}BF_{10}NP$ : C 60.28, H 4.48, N 2.01; found: C 60.27, H 4.61, N 2.25.

**21:** Compound **4** was prepared in situ by dissolving equivalent amounts of dimethylcyclopentenylphosphane (**5**) (100.0 mg, 0.297 mmol) and bis(pentafluorophenyl)borane (102.5 mg, 0.296 mmol) in  $[D_2]$ dichloromethane (4 mL) and stirring for ca. 5 min at r.t. The solution was cooled to  $-78^\circ C$ , the flask evacuated, and  $CO$  gas (2 bar) pressed on it for 5 min with stirring. The stirring was stopped, and the light yellow solution layered with *n*-pentane (3 mL). The reaction mixture was kept under a  $CO$  atmosphere at  $-40^\circ C$ . After several days product **21** was obtained as yellow crystalline material (110.4 mg, 0.155 mmol, 52%). The obtained crystals were suitable for the X-ray crystal structure analysis. Elemental analysis calcd for  $C_{36}H_{30}BF_{10}OP$ : C 60.87, H 4.26; found: C 60.53, H 4.67.

### Reaction with nitrogen monoxide

**22:** Compound **4** was prepared in situ by dissolving equivalent amounts of dimethylcyclopentenylphosphane (**5**) (100.0 mg, 0.297 mmol) and bis(pentafluorophenyl)borane (102.8 mg, 0.297 mmol) in *n*-pentane (6 mL) and stirring at r.t. for ca. 10 min. The solution was degassed, cooled to  $-78^\circ C$ , and  $NO$  gas (2 bar) pressure was applied for a few minutes, upon which a brownish precipitate was formed. The reaction mixture was allowed to warm to r.t. and stirred for another 5 min. Excess  $NO$  gas was removed by flushing with argon gas, upon which the precipitate turned turquoise. The solvent was removed by filter cannula, the residue washed with *n*-pentane (2  $\times$  3 mL), and dried in vacuo. Compound **22** was obtained as light turquoise powder (176.8 mg, 0.248 mmol, 83%). Single crystals of compound **22** suitable for the X-ray crystal structure analysis were obtained by slow diffusion of cyclopentane into a solution of the obtained light turquoise solid in  $CH_2Cl_2$  at  $-40^\circ C$ . Elemental analysis calcd for  $C_{35}H_{30}BF_{10}NOP$ : C 59.01, H 4.24, N 1.97; found: C 59.04, H 4.11, N 1.90.

### Reaction with dihydrogen

**27:** Compound **26** (82.2 mg, 0.078 mmol) was suspended in  $CH_2Cl_2$  (3.5 mL) and the reaction mixture stirred under an atmosphere of  $H_2$  gas (50 bar) at r.t. for 30 h. Purification by filtration over silica and crystallization from a concentrated  $CH_2Cl_2$  solution at  $-40^\circ C$  gave compound **27** as white crystalline material (42.3 mg, 0.040 mmol, 51%). The obtained crystals were suitable for the X-ray crystal structure analysis. Elemental analysis calcd for  $C_{48}H_{33}B_2F_{20}OP\cdot CH_2Cl_2$ : C 51.48, H 3.09; found: C 51.44, H 3.00.

### Formylborane chemistry

**28:** Compound **26** (354 mg, 0.335 mmol) was suspended in  $CH_2Cl_2$  (8 mL) and excess pyridine (0.15 mL, 1.86 mmol, 5.2 equiv) was added, and the reaction mixture stirred at r.t. for 3 h. Separation of the formylborane **28** and the FLP-pyridine adduct **8** by filtration over silica and crystallization from a concentrated toluene/*n*-pentane solution at  $-40^\circ C$  gave compound **28** as off-white crystalline material (101.8 mg, 0.225 mmol, 67%).

### Wittig olefination

**30:** Compound **28** (54.2 mg, 0.120 mmol) and ethyldentriphenylphosphorane (34.7 mg, 0.120 mmol) were dissolved in THF and stirred at r.t. for 5.5 h. Purification by column chromatography gave compound **30** as an off-white, highly viscous oil (26.5 mg, 0.0570 mmol, 48%).

### Imine formation

**31:** Compound **28** (50.3 mg, 0.111 mmol) was dissolved in  $CD_2Cl_2$  (0.7 mL), aniline (10.3 mg, 0.111 mmol) dissolved in  $CD_2Cl_2$  (0.7 mL) was added, and the reaction mixture stirred over  $MgSO_4$  for 2 days at r.t. The suspension was filtered through a Whatman filter and analyzed by NMR spectroscopy. Compound **31** was obtained by crystallization from  $CD_2Cl_2/n$ -pentane at  $-40^\circ C$  as white crystalline material (31.6 mg, 0.0598 mmol, 54%). The obtained crystals were suitable for the X-ray crystal structure analysis. Elemental analysis calcd for  $C_{24}H_{11}BF_{10}N_2$ : C 54.58, H 2.10, N 5.30; found: C 54.33, H 2.05, N 5.22.

CCDC 1457831, 1457832, 1457833, 1457834, 1457835, 1457836, 1457837, 1457838, 1457839, 1457840, 1457841, 1457842, 1457843, 1457844, 1457845, 1457856, 1457847, 1457848, 1457849 and

1457850 contain the supplementary crystallographic data for this paper. These data can be obtained free of charge from The Cambridge Crystallographic Data Centre.

## Acknowledgements

Financial support from the Deutsche Forschungsgemeinschaft is gratefully acknowledged. T.H.W. is grateful to the US National Science Foundation (CHE-1459090).

**Keywords:** boron • CO reduction • dihydrogen splitting • frustrated Lewis pairs • nitroxide radicals • phosphorus

- [1] a) D. W. Stephan, G. Erker, *Angew. Chem. Int. Ed.* **2015**, *54*, 6400–6441; *Angew. Chem.* **2015**, *127*, 6498–6541; b) *Frustrated Lewis Pairs I, Uncovering and Understanding* (Eds: D. W. Stephan, G. Erker), *Topics Curr. Chem.* **2013**, *332*, Springer, Heidelberg; c) *Frustrated Lewis Pairs II, Expanding the Scope, Topics Curr. Chem.* **2013**, *334*, Springer, Heidelberg.
- [2] Other recent reviews: a) A. L. Kenward, W. E. Piers, *Angew. Chem. Int. Ed.* **2008**, *47*, 38–41; *Angew. Chem.* **2008**, *120*, 38–42; b) D. W. Stephan, *Org. Biomol. Chem.* **2008**, *6*, 1535–1539; c) D. W. Stephan, *Dalton Trans.* **2009**, 3129–3136; d) D. W. Stephan, *Chem. Commun.* **2010**, *46*, 8526–8533; e) D. W. Stephan, *Acc. Chem. Res.* **2015**, *48*, 306–316; f) D. W. Stephan, *J. Am. Chem. Soc.* **2015**, *137*, 10018–10032; g) J. M. Bayne, D. W. Stephan, *Chem. Soc. Rev.* **2016**, *45*, 765–774.
- [3] G. C. Welch, D. W. Stephan, *J. Am. Chem. Soc.* **2007**, *129*, 1880–1881.
- [4] a) T. A. Rokob, A. Hamza, A. Stirling, T. Soós, I. Pápai, *Angew. Chem.* **2008**, *120*, 2469–2472; b) S. Grimme, H. Kruse, L. Goerigk, G. Erker, *Angew. Chem. Int. Ed.* **2010**, *49*, 1402–1405; *Angew. Chem.* **2010**, *122*, 1444–1447; c) T. A. Rokob, I. Pápai, *Top. Curr. Chem.* **2013**, *332*, 157–211; d) B. Schirmer, S. Grimme, *Top. Curr. Chem.* **2013**, *332*, 213–230.
- [5] a) D. J. Parks, W. E. Piers, *J. Am. Chem. Soc.* **1996**, *118*, 9440–9441; b) G. Erős, H. Mehdi, I. Pápai, T. A. Rokob, P. Király, G. Tárkányi, T. Soós, *Angew. Chem. Int. Ed.* **2010**, *49*, 6559–6563; *Angew. Chem.* **2010**, *122*, 6709–6713; c) M. M. Morgan, A. J. V. Marwitz, W. E. Piers, M. Parvez, *Organometallics* **2013**, *32*, 317–322; d) D. J. Scott, M. J. Fuchter, A. E. Ashley, *Angew. Chem. Int. Ed.* **2014**, *53*, 10218–10222; *Angew. Chem.* **2014**, *126*, 10382–10386; e) V. Morozova, P. Mayer, G. Berionni, *Angew. Chem. Int. Ed.* **2015**, *54*, 14508–14512; *Angew. Chem.* **2015**, *127*, 14716–14720; f) S. Tussing, K. Kaupmees, J. Paradies, *Chem. Eur. J.* **2016**, *22*, 7422–7426.
- [6] a) M. Alcarazo, C. Gomez, S. Holle, R. Goddard, *Angew. Chem. Int. Ed.* **2010**, *49*, 5788–5791; *Angew. Chem.* **2010**, *122*, 5924–5927; b) E. L. Kolychev, T. Bannenberg, M. Freytag, C. G. Daniliuc, P. G. Jones, M. Tamm, *Chem. Eur. J.* **2012**, *18*, 16938–16946; c) S. R. Flynn, O. J. Metters, D. F. Wass, *Organometallics* **2016**, *35*, 847–850; d) E. R. Clark, A. D. Gross, M. J. Ingleson, *Chem. Eur. J.* **2013**, *19*, 2462–2466; e) M. Devillard, R. Brousses, K. Miqueu, G. Bouhadir, D. Bourissou, *Angew. Chem. Int. Ed.* **2015**, *54*, 5722–5726; *Angew. Chem.* **2015**, *127*, 5814–5818; f) T. vom Stein, M. Peréz, R. Dobrovetsky, D. Winkelhaus, C. B. Caputo, D. W. Stephan, *Angew. Chem. Int. Ed.* **2015**, *54*, 10178–10182; *Angew. Chem.* **2015**, *127*, 10316–10320; g) P. Eisenberger, B. P. Bestvater, E. C. Keske, C. M. Crudden, *Angew. Chem. Int. Ed.* **2015**, *54*, 2467–2471; *Angew. Chem.* **2015**, *127*, 2497–2501.
- [7] a) X. Fan, J. Zheng, Z. H. Li, H. Wang, *J. Am. Chem. Soc.* **2015**, *137*, 4916–4919; b) D. J. Scott, M. J. Fuchter, A. E. Ashley, *J. Am. Chem. Soc.* **2014**, *136*, 15813–15816; c) T. Mahdi, D. W. Stephan, *J. Am. Chem. Soc.* **2014**, *136*, 15809–15812; d) C. Jiang, D. W. Stephan, *Dalton Trans.* **2013**, *42*, 630–637; e) Y. Segawa, D. W. Stephan, *Chem. Commun.* **2012**, *48*, 11963–11965.
- [8] G. C. Welch, R. R. S. Juan, J. D. Masuda, D. W. Stephan, *Science* **2006**, *314*, 1124–1126.
- [9] P. Spies, G. Erker, G. Kehr, R. Fröhlich, S. Grimme, D. W. Stephan, *Chem. Commun.* **2007**, 5072–5074.
- [10] a) R. Roesler, W. E. Piers, M. Parvez, *J. Organomet. Chem.* **2003**, *680*, 218–222; b) K. Chernichenko, M. Nieger, M. Leskelä, T. Repo, *Dalton Trans.* **2012**, *41*, 9029–9032; further see: c) K. Chernichenko, B. Kótai, I. Pápai, V. Zhivonitko, M. Nieger, M. Leskelä, T. Repo, *Angew. Chem. Int. Ed.* **2015**, *54*, 1749–1753; *Angew. Chem.* **2015**, *127*, 1769–1773; d) M.-A. Legare, M.-A. Courtemanche, É. Rochette, F.-G. Fontaine, *Science* **2015**, *349*, 513–516; e) K. Chernichenko, Á. Madarász, I. Pápai, M. Nieger, M. Leskelä, T. Repo, *Nat. Chem.* **2013**, *5*, 718–723; f) K. Chernichenko, M. Lindqvist, B. Kótai, M. Nieger, K. Sorochkina, I. Pápai, T. Repo, *J. Am. Chem. Soc.* **2016**, *138*, 4860–4868.
- [11] a) M. Lindqvist, K. Borre, K. Axenov, B. Kótai, M. Nieger, M. Leskelä, I. Pápai, T. Repo, *J. Am. Chem. Soc.* **2015**, *137*, 4038–4041; b) Z. Mo, E. L. Kolychev, A. Rit, J. Campos, H. Niu, S. Aldridge, *J. Am. Chem. Soc.* **2015**, *137*, 12227–12230; c) M. A. Dureen, D. W. Stephan, *J. Am. Chem. Soc.* **2010**, *132*, 13559–13568; d) L. Keweloh, H. Lockerr, E.-U. Würthwein, W. Uhl, *Angew. Chem. Int. Ed.* **2016**, *55*, 3212–3215; *Angew. Chem.* **2016**, *128*, 3266–3269; e) K. Samigullin, I. Georg, M. Bolte, H.-W. Lerner, M. Wagner, *Chem. Eur. J.* **2016**, *22*, 3478–3484. Also see: f) T. Holtrichter-Rößmann, C. Rösener, J. Hellmann, W. Uhl, E.-U. Würthwein, R. Fröhlich, B. Wibbeling, *Organometallics* **2012**, *31*, 3272–3283.
- [12] T. Özgün, K. Bergander, L. Liu, C. G. Daniliuc, S. Grimme, G. Kehr, G. Erker, *Chem. Eur. J.* **2016**, *22*, 11958–11961.
- [13] We had previously reported the CO/borane reduction at the in situ generated FLP **4**, but at that time could not isolate nor characterize this P/B FLP other than by its clean CO/HB(C<sub>6</sub>F<sub>5</sub>)<sub>2</sub> reaction: M. Sajid, L.-M. Elmer, C. Rosorius, C. G. Daniliuc, S. Grimme, G. Kehr, G. Erker, *Angew. Chem. Int. Ed.* **2013**, *52*, 2243–2246; *Angew. Chem.* **2013**, *125*, 2299–2302.
- [14] a) E. A. Braude, J. A. Coles, *J. Chem. Soc.* **1950**, 2014–2019; b) E. A. Braude, W. F. Forbes, *J. Chem. Soc.* **1951**, 1755–1761.
- [15] a) D. J. Parks, D. J. von H. Spence, W. E. Piers, *Angew. Chem. Int. Ed. Engl.* **1995**, *34*, 809–811; *Angew. Chem.* **1995**, *107*, 895–897; b) D. J. Parks, W. E. Piers, G. P. A. Yap, *Organometallics* **1998**, *17*, 5492–5503.
- [16] a) H. Wang, R. Fröhlich, G. Kehr, G. Erker, *Chem. Commun.* **2008**, 5966–5968; b) P. Spies, S. Schwendemann, S. Lange, G. Kehr, R. Fröhlich, G. Erker, *Angew. Chem. Int. Ed.* **2008**, *47*, 7543–7546; *Angew. Chem.* **2008**, *120*, 7654–7657; c) S. Schwendemann, R. Fröhlich, G. Kehr, G. Erker, *Chem. Sci.* **2011**, *2*, 1842–1849.
- [17] a) C. H. Lee, S. J. Lee, J. W. Park, K. H. Kim, B. Y. Lee, J. S. Oh, *J. Mol. Catal. A* **1998**, *132*, 231–239; b) C. M. Mömeling, S. Frömel, G. Kehr, R. Fröhlich, S. Grimme, G. Erker, *J. Am. Chem. Soc.* **2009**, *131*, 12280–12289.
- [18] H. Jacobsen, H. Berke, S. Döring, G. Kehr, G. Erker, R. Fröhlich, O. Meyer, *Organometallics* **1999**, *18*, 1724–1735.
- [19] a) M. A. Dureen, C. C. Brown, D. W. Stephan, *Organometallics* **2010**, *29*, 6594–6607; b) C. Jiang, O. Blacque, H. Berke, *Organometallics* **2010**, *29*, 125–133; c) M. A. Dureen, D. W. Stephan, *J. Am. Chem. Soc.* **2009**, *131*, 8396–8397.
- [20] C. M. Mömeling, G. Kehr, R. Fröhlich, G. Erker, *Dalton Trans.* **2010**, *39*, 7556–7564.
- [21] C. Rosorius, G. Kehr, R. Fröhlich, S. Grimme, G. Erker, *Organometallics* **2011**, *30*, 4211–4219.
- [22] a) C. M. Mömeling, E. Otten, G. Kehr, R. Fröhlich, S. Grimme, D. W. Stephan, G. Erker, *Angew. Chem. Int. Ed.* **2009**, *48*, 6643–6646; *Angew. Chem.* **2009**, *121*, 6770–6773; b) I. Peuser, R. C. Neu, X. Zhao, M. Ulrich, B. Schirmer, J. A. Tannert, G. Kehr, R. Fröhlich, S. Grimme, G. Erker, D. W. Stephan, *Chem. Eur. J.* **2011**, *17*, 9640–9650.
- [23] a) X. Zhao, D. W. Stephan, *Chem. Commun.* **2011**, *47*, 1833–1835; b) K. Takeuchi, D. W. Stephan, *Chem. Commun.* **2012**, *48*, 11304–11306; c) T. Voss, T. Mahdi, E. Otten, R. Fröhlich, G. Kehr, D. W. Stephan, G. Erker, *Organometallics* **2012**, *31*, 2367–2378; d) M. Reißmann, A. Schäfer, S. Jung, T. Müller, *Organometallics* **2013**, *32*, 6736–6744; e) D. Voicu, M. Abolhasani, R. Choueiri, G. Lestari, C. Seiler, G. Menard, J. Greener, A. Günther, D. W. Stephan, E. Kumacheva, *J. Am. Chem. Soc.* **2014**, *136*, 3875–3880; f) Y.-L. Liu, G. Kehr, C. G. Daniliuc, G. Erker, *Chem. Sci.* **2016**, *7*, DOI: 10.1039/C6SC03468C and references cited therein.
- [24] a) A. Stute, G. Kehr, C. G. Daniliuc, R. Fröhlich, G. Erker, *Dalton Trans.* **2013**, *42*, 4487–4499; b) A. Stute, L. Heletta, R. Fröhlich, C. G. Daniliuc, G. Kehr, G. Erker, *Chem. Commun.* **2012**, *48*, 11739–11741; c) A. Stute, G. Kehr, R. Fröhlich, G. Erker, *Chem. Commun.* **2011**, *47*, 4288–4290; d) M. W. P. Bebbington, S. Bontemps, G. Bouhadir, D. Bourissou, *Angew. Chem. Int. Ed.* **2007**, *46*, 3333–3336; *Angew. Chem.* **2007**, *119*, 3397–3400.
- [25] a) H. Staudinger, J. Meyer, *Helv. Chim. Acta* **1919**, *2*, 635–646; b) C. G. Stuckwisch, *Synthesis* **1973**, 469–483; c) E. W. Abel, S. A. Mucklejohn,

- Phosphorus Sulfur Silicon Relat. Elem.* **1981**, *9*, 235–266; d) Y. G. Gololobov, I. N. Zhmurova, L. F. Kasukhin, *Tetrahedron* **1981**, *37*, 437–472; e) Y. G. Gololobov, L. F. Kasukhin, V. S. Petrenko, *Phosphorus Sulfur Silicon Relat. Elem.* **1987**, *30*, 393–396; f) E. F. V. Scriven, K. Turnbull, *Chem. Rev.* **1988**, *88*, 297–368; g) G. Gololobov, L. F. Kasukhin, *Tetrahedron* **1992**, *48*, 1353–1406; h) P. Molina, M. J. Vilaplana, *Synthesis* **1994**, 1197–1218; i) M. Köhn, R. Breibauer, *Angew. Chem. Int. Ed.* **2004**, *43*, 3106–3116; *Angew. Chem.* **2004**, *116*, 3168–3178; j) M. W. P. Bebbington, D. Bourissou, *Coord. Chem. Rev.* **2009**, *293*, 1248–1261.
- [26] a) S. Bittner, M. Pomerantz, Y. Assaf, P. Krief, S. Xi, M. K. Witczak, *J. Org. Chem.* **1988**, *53*, 1–5; b) P. Molina, C. Lopéz-Leonardo, J. Llamas-Botía, C. Foces-Foces, C. Fernandez-Castaño, *J. Chem. Soc. Chem. Commun.* **1995**, 1387–1389; c) J. Kovács, I. Pintér, M. Katjár-Péredy, L. Somsák, *Tetrahedron* **1997**, *53*, 15041–15050; d) A. T. Katritzky, N. M. Khashab, S. Bobrov, *Helv. Chim. Acta* **2005**, *88*, 1664–1675.
- [27] M. Grün, K. Harms, R. Meyer zu Köcker, K. Dehnicke, H. Goessmann, *Z. Anorg. Allg. Chem.* **1996**, *622*, 1091–1096.
- [28] a) S. Bontemps, G. Bouhadir, K. Miqueu, D. Bourissou, *J. Am. Chem. Soc.* **2006**, *128*, 12056–12057; b) J. Grobe, K. Lütke-Brochtrup, B. Krebs, M. Läge, H.-H. Niemeyer, E.-U. Würthwein, *Z. Naturforsch. B* **2006**, *61*, 882–895.
- [29] See, for example: a) W. Hieber, *Die Chemie* **1942**, *55*, 25–28; b) J. Chatt, *Nature* **1950**, *165*, 637–638; c) D. M. P. Mingos, *J. Organomet. Chem.* **2001**, *635*, 1–8. See also: d) K. G. Caulton, R. F. Fenske, *Inorg. Chem.* **1968**, *7*, 1273–1284; e) N. A. Beach, H. B. Gray, *J. Am. Chem. Soc.* **1968**, *90*, 5713–5721.
- [30] a) M. Sajid, A. Lawzer, W. Dong, C. Rosorius, W. Sander, B. Schirmer, S. Grimme, C. G. Daniliuc, G. Kehr, G. Erker, *J. Am. Chem. Soc.* **2013**, *135*, 18567–18574; b) O. Ekkert, G. González Miera, T. Wiegand, H. Eckert, B. Schirmer, J. L. Petersen, C. G. Daniliuc, R. Fröhlich, S. Grimme, G. Kehr, G. Erker, *Chem. Sci.* **2013**, *4*, 2657–2664; for a comparison see: c) T. W. Hudnall, Y. M. Kim, M. W. P. Bebbington, D. Bourissou, F. P. Gabbaï, *J. Am. Chem. Soc.* **2008**, *130*, 10890–10891; d) C.-B. Chiu, F. P. Gabbaï, *Dalton Trans.* **2008**, 814–817; e) T.-P. Lin, P. Gualco, S. Ladeira, A. Amgoune, D. Bourissou, F. P. Gabbaï, *C. R. Chim.* **2010**, *13*, 1168–1172; f) M. A. Courtemanche, M. A. Legare, L. Maron, F. G. Fontaine, *J. Am. Chem. Soc.* **2013**, *135*, 9326–9329.
- [31] a) T. Wiegand, H. Eckert, O. Ekkert, R. Fröhlich, G. Kehr, G. Erker, S. Grimme, *J. Am. Chem. Soc.* **2012**, *134*, 4236–4249; b) T. Wiegand, M. Siedow, H. Eckert, G. Kehr, G. Erker, *Isr. J. Chem.* **2015**, *55*, 150–178.
- [32] J. C. C. Chan, H. Eckert, *J. Magn. Reson.* **2000**, *147*, 170–178.
- [33] N. L. Nichols, C. D. Hause, R. H. Noble, *J. Chem. Phys.* **1955**, *23*, 57–61.
- [34] For a comparison, see: a) A. J. P. Cardenas, B. J. Culotta, T. H. Warren, S. Grimme, A. Stute, R. Fröhlich, G. Kehr, G. Erker, *Angew. Chem. Int. Ed.* **2011**, *50*, 7567–7571; *Angew. Chem.* **2011**, *123*, 7709–7713; b) M. Sajid, A. Stute, A. J. P. Cardenas, B. J. Culotta, J. A. M. Hepperle, T. H. Warren, B. Schirmer, S. Grimme, A. Studer, C. D. Daniliuc, R. Fröhlich, J. L. Petersen, G. Kehr, G. Erker, *J. Am. Chem. Soc.* **2012**, *134*, 10156–10168; c) M. Sajid, G. Kehr, T. Wiegand, H. Eckert, C. Schwickert, R. Pöttgen, A. J. P. Cardenas, T. H. Warren, R. Fröhlich, C. G. Daniliuc, G. Erker, *J. Am. Chem. Soc.* **2013**, *135*, 8882–8895; d) J. C. M. Pereira, M. Sajid, G. Kehr, A. M. Wright, B. Schirmer, Z.-W. Qu, S. Grimme, G. Erker, P. C. Ford, *J. Am. Chem. Soc.* **2014**, *136*, 513–519.
- [35] a) M. de Oliveira Jr., T. Wiegand, M. L. Elmer, M. Sajid, G. Kehr, G. Erker, C. J. Magon, H. Eckert, *J. Chem. Phys.* **2015**, *142*, 124201; b) M. de Oliveira Jr., R. Knitsch, M. Sajid, A. Stute, L.-M. Elmer, G. Kehr, G. Erker, C. J. Magon, G. Jeschke, H. Eckert, *PLoS One* **2016**, *11*, e0157944.
- [36] a) L. B. Volodarsky, V. A. Reznikov, V. I. Ovacharenko, *Synthetic Chemistry of Stable Nitroxides*, CRC Press, Boca Raton, **1994**; b) C. Chang, K. O. Siegenthaler, A. Studer, *Helv. Chim. Acta* **2006**, *89*, 2200–2210; c) G. I. Likhtenstein, J. Yamauchi, S. Nakatsuji, A. I. Smirnov, R. Tamura, *Nitroxide Applications in Chemistry, Biomedicine, and Material Sciences*; Wiley-VCH: Weinheim, Germany, **2008**; d) T. Vogler, A. Studer, *Synthesis* **2008**, 1979–1993; e) S. Miele, P. Nesvadba, A. Studer, *Macromolecules* **2009**, *42*, 2419–2427; f) M. Sajid, G. Jeschke, M. Wiebcke, A. Godt, *Chem. Eur. J.* **2009**, *15*, 12960–12962; g) *Stable Radicals: Fundamentals and Applied Aspects of Odd-Electron Compounds* (Ed. R. G. Hicks) Wiley, Hoboken, **2010**; h) L. Tebben, A. Studer, *Angew. Chem. Int. Ed.* **2011**, *50*, 5034–5068; *Angew. Chem.* **2011**, *123*, 5138–5174.
- [37] K. Matyjaszewski, B. E. Woodworth, X. Zhang, S. G. Gaynor, Z. Metzner, *Macromolecules* **1998**, *31*, 5955–5957.
- [38] a) C. J. Hawker, A. W. Bosman, E. Harth, *Chem. Rev.* **2001**, *101*, 3661–3688; b) V. Sciannamea, R. Jérôme, C. Detrembleur, *Chem. Rev.* **2008**, *108*, 1104–1126; c) M. K. Brinks, A. Studer, *Macromol. Rapid Commun.* **2009**, *30*, 1043–1057.
- [39] a) A. B. Burg, H. I. Schlesinger, *J. Am. Chem. Soc.* **1937**, *59*, 780–787; b) T. P. Fehlner, W. S. Koski, *J. Am. Chem. Soc.* **1965**, *87*, 409–413; c) T. P. Fehlner, G. W. Mappes, *J. Phys. Chem.* **1969**, *73*, 873–882; d) H. Umeyama, K. Morokuma, *J. Am. Chem. Soc.* **1976**, *98*, 7208–7220; e) T. W. Bentley, *J. Org. Chem.* **1982**, *47*, 60–64; f) E. Kaufmann, P. v. R. Schleyer, S. Gronert, A. Streitwieser Jr., M. Halpern, *J. Am. Chem. Soc.* **1987**, *109*, 2553–2559; g) C. W. Bauschlicher Jr., A. Ricca, *Chem. Phys. Lett.* **1995**, *237*, 14–19; h) Catalyzed reaction: M. W. Rathke, H. C. Brown, *J. Am. Chem. Soc.* **1966**, *88*, 2606–2607.
- [40] For a comparison, see: M. Sajid, G. Kehr, C. G. Daniliuc, G. Erker, *Angew. Chem. Int. Ed.* **2014**, *53*, 1118–1121; *Angew. Chem.* **2014**, *126*, 1136–1139.
- [41] a) F. B. Mallory, C. W. Mallory, W. M. Ricker, *J. Am. Chem. Soc.* **1975**, *97*, 4770–4771; b) R. H. Contreras, L. C. Ducati, C. F. Tormena, *Quantum Chem.* **2012**, *112*, 3158–3163; c) C. Chen, M. Harhausen, R. Liedtke, K. Bussmann, A. Fukazawa, S. Yamaguchi, J. L. Petersen, C. D. Daniliuc, R. Fröhlich, G. Kehr, G. Erker, *Angew. Chem. Int. Ed.* **2013**, *52*, 5992–5996; *Angew. Chem.* **2013**, *125*, 6108–6112; d) C. Chen, M. Harhausen, A. Fukazawa, S. Yamaguchi, R. Fröhlich, C. G. Daniliuc, J. L. Petersen, G. Kehr, G. Erker, *Chem. Asian J.* **2014**, *9*, 1671–1681; e) J.-C. Hierso, *Chem. Rev.* **2014**, *114*, 4838–4867; f) R. J. Blagg, E. J. Lawrence, K. Resner, V. S. Oganesyan, T. J. Herrington, A. E. Ashley, G. G. Wildgoose, *Dalton Trans.* **2016**, *45*, 6023–6031.
- [42] M. Sajid, G. Kehr, C. G. Daniliuc, G. Erker, *Chem. Eur. J.* **2015**, *21*, 1454–1457.
- [43] For a comparison, see: a) M. E. D. Hillman, *J. Am. Chem. Soc.* **1962**, *84*, 4715–4720; b) H. C. Brown, *Acc. Chem. Res.* **1969**, *2*, 65–72; c) H. C. Brown, R. K. Bakshi, B. Singaram, *J. Am. Chem. Soc.* **1988**, *110*, 1529–1534; d) M. Yalpani, R. Köster, *J. Organomet. Chem.* **1992**, *434*, 133–141; e) G. W. Kabalka, J. T. Gotsick, R. D. Pace, N.-S. Li, *Organometallics* **1994**, *13*, 5163–5165; f) V. K. Aggarwal, G. Y. Fang, X. Ginesta, D. M. Howells, M. Zaja, *Pure Appl. Chem.* **2006**, *78*, 215–229; g) A. Fukazawa, J. L. Dutton, C. Fan, L. G. Mercier, A. Y. Houghton, Q. Wu, W. E. Piers, M. Parvez, *Chem. Sci.* **2012**, *3*, 1814–1818.
- [44] K. V. Axenov, C. M. Mömming, G. Kehr, R. Fröhlich, G. Erker, *Chem. Eur. J.* **2010**, *16*, 14069–14073.

Received: August 22, 2016

Revised: September 23, 2016

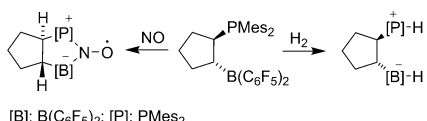
Published online on ■■■, 0000

## FULL PAPER

### Frustrated Lewis Pairs

L.-M. Elmer, G. Kehr, C. G. Daniliuc,  
M. Siedow, H. Eckert, M. Tesch, A. Studer,  
K. Williams, T. H. Warren, G. Erker\*

■ ■ - ■ ■



**Poised to attack:** The *trans*-1,2-attachment of the  $\text{B}(\text{C}_6\text{F}_5)_2$  and  $\text{PMes}_2$  functional groups at a cyclopentane framework leads to a non-interacting frustrated P/B Lewis pair (see Scheme). The diverse reactivity of this system was studied in detail.

 The Chemistry of a Non-Interacting  
Vicinal Frustrated Phosphane/Borane  
Lewis Pair